COMPARING METHODS FOR ESTIMATING MANNING'S ROUGHNESS COEFFICIENT ON A PORTION OF THE SOUTH FORK OF CHESTER CREEK

By

Grant A. Warnke, B.S.C.E.

A Project Submitted in Partial Fulfillment of the Requirements

for the Degree of

MASTER OF SCIENCE

in

Civil Engineering

University of Alaska Anchorage

May 2018

APPROVED:

Rob Lang, Ph.D., Committee Chair
Tom Ravens, Ph.D., Committee Member
John Bean, M.S., Committee Member

Joey Yang, Ph.D., Chair
Department of Civil Engineering
Fred Barlow, Ph.D., Dean
College of Engineering

a

Table of Contents

Table of Figures

List of Tables

Table of Equations

Abstract

This report compares several different methods used for estimating the Manning roughness coefficient of a reach using observed conditions during spring runoff. A survey was taken of the South Fork of Chester Creek in the small valley between the Engineering and Computation Building and the North-West Parking Lot at UAA. The survey included 16 cross sections, a center line profile, water surface elevations (WSE's), and flow velocity readings at each cross section. Based on observed conditions, a model was created in HEC-RAS to calculate the hydraulic characteristics at each cross section. These hydraulic characteristics, along with downstream cross section lengths and head losses, were used to calculate the composite roughness of the reach. This value was then compared to a visual method that accounts for flow-retarding factors, and an empirical method developed in a laboratory. The roughness values computed for the analytical, empirical, and visual methods were 0.071, 0.045, and 0.077 respectively. Additionally, the three computed coefficients were compared with two methods that involve matching table values. The two approximate table values were 0.11 and 0.10. Supplementary methods not used in the analysis are also discussed.

1.0 Introduction

The point of hydraulic and hydrologic studies is to determine the hydrodynamics of a basin. More specifically, stream discharges and flood water elevations are desired. Determining the flow capacity of a channel is a very difficult and complex task due to the nature of natural channels. They are highly dynamic systems that can vary on the scale of hours. As a result, the equations used to describe open channel flow become exceedingly difficult to solve and implement correctly. Even if the equations were solved correctly, it would take an unrealistic amount of time to perform the calculations. However, with the advent of numerical methods and computers, professional practicing engineers use a computational software of their choice to solve these complex problems. The US Army Corps of Engineers' (USACE) software, Hydrologic Engineering Center – River Analysis System (HEC-RAS), is arguably the most widely used simulation tool for hydraulic calculations.

HEC-RAS uses the standard step backwater curve method when running 1D steady flow models (including gradually varied flow, or GVF). More specifically, it uses the secant method (a numerical method) to solve the equation for GVF in the form of a conservation of energy equation (Strum, 2009) that looks like the following:

Equation 1. Energy equation for GVF

$$WS_2 + \alpha_2 \frac{V_2^2}{2g} = WS_1 + \alpha_1 \frac{V_1^2}{2g} + h_e$$

Equation 2. Head loss due to contraction and expansion

$$h_e = \bar{S_e} L + K_L \left| \frac{\alpha_2 V_2^2}{2g} - \frac{\alpha_1 V_1^2}{2g} \right|$$

Where WS is the WSE, α is a velocity weighting coefficient, V is velocity, g is the acceleration due to gravity, h_e is the head loss, S_e is the mean slope of the energy grade line, L is the reach length, and K_L is the minor head loss coefficient. A distance weighted reach length is used for L, and is calculated with the following:

Equation 3. Weighted reach length

$$L = \frac{L_{lob} Q_{lob} + L_{ch} Q_{ch} + L_{rob} Q_{rob}}{Q_{lob} + Q_{ch} + L_{rob}}$$

Where the lob, ch, and rob coefficients stand for left of bank, channel, and right of bank respectively, and Q is the volumetric flow rate.

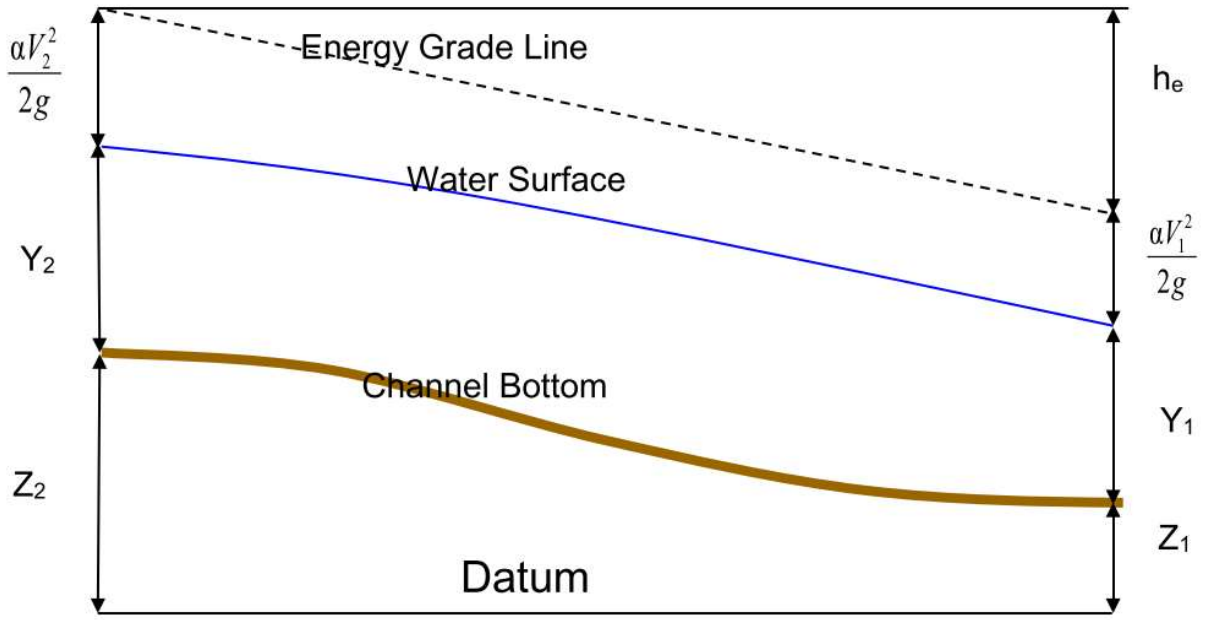

Figure 1. Definition sketch for the standard step method (US Army Corps of Engineers, 2016)

It may not be readily apparent, but each of these equations is a function of the discharge, Q. Given this, the discharge needs to be known in order to use the other equations. Like any water resource engineer, HEC-RAS uses the most famous equation in hydraulics to calculate the flow, Manning's equation. The Manning equation is an empirical equation expressed as follows:

Equation 4. Manning's equation

$$Q = \frac{K_n}{n} A R^{2/3} S_f^{1/2} \left(dimensions: \frac{L^3}{T} \right)$$

Where K_n is a unit coefficient (1.486 when using US customary units and 1 when using SI units), n is the manning roughness coefficient, A is the cross-sectional area perpendicular to the direction of flow, R is the hydraulic radius (the hydraulic radius is equal to the cross-sectional area divided by the wetted perimeter), and S_f is the friction slope. The friction slope is the slope of the head loss, but under gradual or steady state conditions it is estimated to equal the bed slope, S. Additionally, it is important to note that the units of the inputs must all be the same (i.e. if the area is m^2, then the hydraulic radius must be m) due to the equation being empirical. Lastly, it can be seen that n represents a non-dimensional, numerical representation of the ability for a channel to resist flow. Hence the name Manning's roughness coefficient.

An initial Q is used as an input in the case of a steady flow analysis. However, HEC-RAS uses Manning's equation to calculate Q as it changes at the different computational steps when

performing the backwater curve calculation. Consequently, the variables used in the Manning equation must be known.

Besides n, Manning's equation relies entirely on channel bathymetry and profile. These hydraulic characteristics of a channel are easily obtained when conducting field surveys. However, n is much more difficult to calculate. The Manning roughness can rely on many different factors, such as bed forms, bed makeup, channel obstructions, and the flow itself. In this, it has been shown that n becomes a very important input when running hydraulic computations due to the difficulty in estimating it. Different values of n can change the results to a model drastically, so it is imperative to be able to estimate a roughness coefficient that accurately represent field conditions. It is also important to note that the steady flow analysis is not the only analysis that relies on a proper n value. Given that the frictional bed resistance is the same for unsteady flow and steady flow, the Manning equation is used in HEC-RAS to evaluate the mean boundary shear stress during unsteady flow simulations. This includes 1D or 2D applications. The Manning equation is also used when analyzing a channel with ice covers. Ice even has its own Manning roughness coefficient (US Army Corps of Engineers, 2016).

The overarching takeaway from this is that estimating the Manning roughness coefficient is critical to creating an accurate model. Ever since Manning's equation was formulated, a myriad of techniques for estimating n have been studied and developed. These techniques include analytical methods, empirical methods, and visual methods. This is good news when it comes to water resource engineers because not every project is the same. Project limitations can force engineers to use one method over another. For instance, a lack of information might mean that a visual or empirical method must be used over an analytical method. Regardless, it is important to compare the different methods in an academic setting. Without comparing the methods, it is difficult to confirm their validity.

The scope of this project is to compare one of the methods in each category. For the analytical method, a composite roughness coefficient will be developed based on data at each cross section. The empirical method will also use data at each cross section to come up with a composite roughness coefficient over the reach. For the last method, a famous and well documented visual method will be used to come up with a composite roughness. Each value will then be compared to solutions from studies with similar hydraulic properties and conditions.

2.0 Literature Review

A bulk of research exists for estimating a roughness coefficient of a channel. However, generating a value is heavily site specific. There is no one size fits all solution when it comes to developing a Manning roughness for a reach due to the wide variation in variables between sites. Nonetheless, the studies that exist often present many different and valid ways to develop a value. It is up to the investigator to determine which method is best suited for their needs and/or project limitations.

2.1 Published Manning Roughness Coefficients

Chow presents a wide range of roughness coefficients in his book *Open-Channel Hydraulics* (as cited in Strum, 2009, pp. 130-134). These values are very useful when it comes to developing a preliminary roughness, or if a quick estimate is needed. It turns out that this table is still widely used in many professional reports, studies, and even government developed engineering manuals (Oregon Department of Transportation - Highway Division, 2014). Chow's table can be seen in section 8.1 of the Appendix.

2.2 Published Analytic Methods

Most of the time, roughness coefficients vary form cross section to cross section. Therefore, it would behoove one's self to develop a composite roughness for the reach to simplify calculations. Barnes, Jarrett, and Petsch derived the equation to calculate a composite roughness coefficient for a reach from Equation 4, the Manning equation (as cited in Coon, 1998). The equation requires a known discharge, the water surface profiles, and hydraulic properties of the reach at each cross section. The nature of the equation is described fully in the methodology section of this paper.

2.3 Published Empirical Methods

A litany of experiments have been conducted on the Manning roughness coefficient since the 60's. The empirical relationships developed in these studies can be very useful for assessing the accuracy of a model. Limerinos used 11 sites in California to develop a relationship for the roughness, hydraulic radius, and particle size (as cited in Coon, 1998). The main goal was to choose a representative channel that did not affect the roughness with its geometry. Instead,

Limerinos sought to isolate the effect of the bed roughness. In doing so, the following relationship was developed:

Equation 5. Limerinos' relationship between roughness, hydraulic radius, and particle size

$$n = \frac{(0.0926)R^{1/6}}{1.16 + 2.0\log\left(\frac{R}{d_{84}}\right)}$$

Where R is the hydraulic radius in feet and d_{84} is the particle diameter in feet that is larger than or equal to 84% of the particle sizes in a grain size distribution. Additionally, Henderson and Froehlich also came up with their own relationships relating the roughness with particle size (as cited in Coon, 1998). These equations can be seen below in the form of Equation 6 and Equation 7.

Equation 6. Henderson's equation developed in 1966

$$n = 0.034 d_{50}^{1/6}$$

Equation 7. Froelich's equation developed in 1978

$$n = 0.245 R^{0.14} \left(\frac{R}{d_{50}}\right)^{-0.44} (R/T)^{0.30}$$

Where d_{50} is the particle diameter that is larger than or equal to 50% of the particle sizes in a grain size distribution, R is the hydraulic radius, and T is the top width of a stream all in US customary units. Henderson's equation is based on data collected from gravel bed streams, while Froelich's equation is based on data collected from an outside source and is subject to limitations. This data was collected by Barnes (as cited in Coon, 1998) and is germane to water surface slopes between 0.0003 and 0.018 and hydraulic radii up to 19 ft.

In the case that one does not have data about the bed makeup, empirical relationships that do not involve grain size also exist. Bray and Sauer both came up with their own relationships relating the roughness to the water surface slope (as cited in Coon, 1998). The empirical relationships take the following form:

Equation 8. Bray's equation developed in 1979

$$n = 0.104 S_w^{0.177}$$

Equation 9. Sauer's equation developed in 1990

$$n = 0.11 S_w^{0.18} R^{0.08}$$

Where S_w is the water surface slope and R is the hydraulic radius all in US customary units. Bray's equation was developed in accordance with channels with gravel beds, minimal bed transport, no significant channel bed vegetation, and no dominating bedforms. Additionally, it should be noted that Equation 9 is based on the same data as Equation 7. Therefore, Equation 9 has the same limitations as Equation 7.

One last important relationship, developed by Jarrett (as cited in Coon, 1998), used data from 75 flow rates with 21 different cross sections for cobble and boulder bed mountain streams in Colorado. Instead of relating the water surface slope to the roughness coefficient, Jarrett related it to the energy gradient. Equation 10 shows this relationship, where S_f is the energy gradient in feet per foot and R is the hydraulic radius in feet. Jarrett warns that this relationship is only applicable for channels with energy gradients of 0.002 to 0.09 and hydraulic radii from 0.5 ft to 7 ft.

Equation 10. Jarrett's equation developed in 1984

$$n = 0.39 S_f^{0.38} R^{-0.16}$$

2.4 Published Visual Methods

As previously stated, using already published coefficients is a painless way to develop an initial roughness coefficient. In the same vein, methods based on visual observations can be used to develop an initial n value as well. Hicks and Mason performed a comprehensive study that found roughness coefficients for many different types of channels at different flows in New Zealand using the analytical method previously presented (Hicks & Mason, 1998). From this, they created a book which can be used to compare field observations to their own and match a resulting n value. They suggest matching a reference reach to the one being studied by comparing hydraulic properties and bed properties. However, it is also suggested that visual matching is important. A visual comparison is often the first line of defense when it comes to validating a Manning's n value. If it can't pass the visual test, then it won't pass the other tests.

Although comparing photographs may be a valid initial method, it is used more for flood plain analysis. Calculating the resistance to flow for a flood plain is more difficult due to its variations in elevation, make up, and obstructions. A report published by USGS presents a catalogue of flood plain photographs a long with their roughness values (Arcement & Schneider, 1989). The

report suggests that the photographs can be compared with other investigated reaches to verify computed values or assign initial ones.

A hybrid visual method developed by Cowan adjusts an initial, base n value in accordance with other flow-retarding factors (as cited in Coon, 1998). These factors are all based on visual observations. This famous method is of particular importance and will be discussed further in the methodology section of this report.

2.5 Published Calibration Methods

The most ideal case to have during a study is a complete data set. More specifically, channel geometry, bathymetry at each cross section, and rating curves at each cross section are known. The most important point here is the rating curve. This is because Manning roughness is a function of flow. Flows change dramatically depending on the time of year, especially in climates far from the equator. As the flow changes, the roughness must change as well to maintain the channel's resistance to flow. Due to this variability, it is pertinent to have flow data for all seasons in a year. Additionally, a more complete set of data would include historical data so that a more accurate representation of what is happening can be achieved.

A study conducted for the Juqueriquere River basin used similar data to calibrate an n value in HEC-RAS (Boulomytis, Zuffo, Filho, & Imteaz, 2017). More specifically, a Manning roughness coefficient is developed at each cross section by trial and error given known hydraulic properties, discharges, and WSE's. In HEC-RAS, a steady flow analysis is run on the cross section in question with the correct flow rate. The n value is changed during each run until the observed WSE is achieved in the model. The limitations with this method revolve around data and time.

Some projects can be very large in scope, which means a lot of cross sectional data. In HEC-RAS, running an analysis only requires upstream, downstream, or junction boundary conditions. However, this calibration method requires splitting the reach into tiny reaches (i.e. each cross section). This is due to the effect n has on upstream and downstream conditions. It is near impossible to iterate n values for a reach with multiple cross sections in HEC-RAS and develop the correct observed WSE at each cross section. For example, changing the n value at cross section 7 of a 17-cross section model will possibly change the WSE at all the previous and proceeding cross sections. This volatility in n is due to HEC-RAS using numerical methods to solve the backwater curve. Essentially, the nature of the calculation schemes develops a cross

sectional dependency where variables at each cross section depend on the same variables at other cross sections. As a result, the iteration/refinement process for n is very tedious in the program and zeroing in on a solution becomes next to impossible for a reach with abundant cross sections. Therefore, cross sections are separated into mini reaches with only one cross sectional geometry at the upstream and downstream boundaries to ensure they do not affect each other. This means that boundary conditions must be set for each one. This is tedious, computationally heavy, and inefficient when it comes to large projects. With that being said, it is still a very reliable method in theory when compared to some of the previously presented empirical methods. Consequently, this method is meant more for smaller projects or subsections of a large reach where it is difficult to estimate a roughness.

2.6 Local Effects

The Municipality of Anchorage Alaska is looking into rehabilitating Chester Creek after years of mistreatment. Currently, only a draft report exists, but major plans are in the works (Anchorage Waterways Council, 2014). Future solutions may require the knowledge of roughness coefficients for the watershed. This project may aid the researchers and engineers when assigning such values, especially in the area surrounding the UAA (University of Alaska Anchorage) campus where this study is being conducted.

3.0 Methodology

The calculation of an n value using the analytical method is based solely on the theory and properties of open channel hydraulics. Regardless, no study can be completed without collecting data. Field measurement techniques and their accuracy become important to the validity of a study. In the end, combining the known principles and data collection ultimately allows for the correct application of said principles.

3.1 Hydraulic Principles

As stated before, the most widely used uniform-flow equation is Equation 1, Manning's equation. Although the equation has already been presented, it can be seen below as a reminder.

$$Q = \frac{1.486}{n} A R^{2/3} S_f^{1/2}$$

Where Q is the discharge, in ft^3/s (cfs), A is the wetted channel cross sectional area in ft^2, R is the hydraulic radius in ft, and S_f is the friction slope in ft/ft. However, the friction slope can be expressed as the following:

Equation 11. Friction slope

$$S_f = \frac{h_f}{L} = \frac{\Delta h + \Delta h_v - k(\Delta h_v)}{L}$$

Equation 12. Velocity head

$$h_v = \frac{\alpha V^2}{2g}$$

Equation 13. The continuity equation

$$Q = VA$$

Where h_f is the head loss due to boundary friction along the reach, L is the reach length, Δh is the change in elevation of the water surface between the upstream and downstream cross sections, Δh_v is the change in velocity head between the upstream and downstream cross sections, and $k(\Delta h_v)$ estimates the energy loss due to acceleration or deceleration in a contracting or expanding reach. Chow set the convention that k is 0 for contracting reaches and 0.5 for expanding reaches (as cited in Hicks & Mason, 1998). The velocity head can be calculated using Equation 12, where α is the velocity head coefficient, V is the mean velocity, and g is the acceleration due to gravity, all in US customary units. Hicks and Mason suggest α be equal to 1.0, "This maintains

consistency with previous workers who have presented roughness coefficient data (e.g. Chow, 1959; Barnes, 1963; Jarrett, 1984) and with the application of the slope-area method to channels with simple cross sections." (Hicks & Mason, 1998, p. 5). It is worth noting that the determination of the kinetic energy coefficient (another name for α) is outlined in a study by the USGS (Hulsing, Smith, & Cobb, 1966). However, determining an exact value of α is out of the scope of this study.

With the underlying principles set, a representative n value may be calculated for a multi-section reach at a given discharge. This composite n value is the previously discussed analytical method adopted by Barnes and Jarrett (as cited in Hicks & Mason, 1998). This is done by breaking Equation 1 into cross sections and weighting them based on their geometry and length. This can be done by the following:

$$S_f = \frac{h_f}{L} = \frac{h_{f_{1.2}} + h_{f_{2.3}} + \cdots + h_{f_{(m-1).m}}}{L_{1.2} + L_{2.3} + \cdots + L_{(m-1).m}} = \frac{(h_m - h_1) + \left(h_{v_m} - h_{v_1}\right) - (k_{1.2}\Delta h_{v_{1.2}} + \cdots + k_{(m-1).m}\Delta h_{v_{(m-1).m}})}{L_{1.2} + \cdots + L_{(m-1).m}}$$

$$AR^{2/3} = Z$$

$$\therefore Q = \frac{1.486}{n} Z S_f^{1/2} \rightarrow S_f = \frac{1}{1.486^2}\frac{Q^2 n^2}{Z^2}$$

$$\therefore \frac{(h_m - h_1) + \left(h_{v_m} - h_{v_1}\right) - (k_{1.2}\Delta h_{v_{1.2}} + \cdots + k_{(m-1).m}\Delta h_{v_{(m-1).m}})}{L_{1.2} + \cdots + L_{(m-1).m}} = \frac{1}{1.486^2}\frac{Q^2 n^2}{(Z_1 Z_2 + \cdots + Z_{(m-1)} Z_m)}$$

Equation 14. Analytical equation for estimating a Manning's n value

$$n = \frac{1.486}{Q}\left(\frac{(h_m - h_1) + \left(h_{v_m} - h_{v_1}\right) - (k_{1.2}\Delta h_{v_{1.2}} + \cdots + k_{(m-1).m}\Delta h_{v_{(m-1).m}})}{\frac{L_{1.2}}{Z_1 Z_2} + \cdots + \frac{L_{(m-1).m}}{Z_{(m-1)} Z_m}}\right)^{1/2}$$

Where m is the number of cross sections. Figure 2 presents a definition sketch of this equation. It can be seen that Figure 2 is very similar to Figure 1, which depicts the standard step method used by HEC-RAS to calculate water surface elevations. The juxtaposition of the two figures makes sense because both are based on the same hydraulic principles.

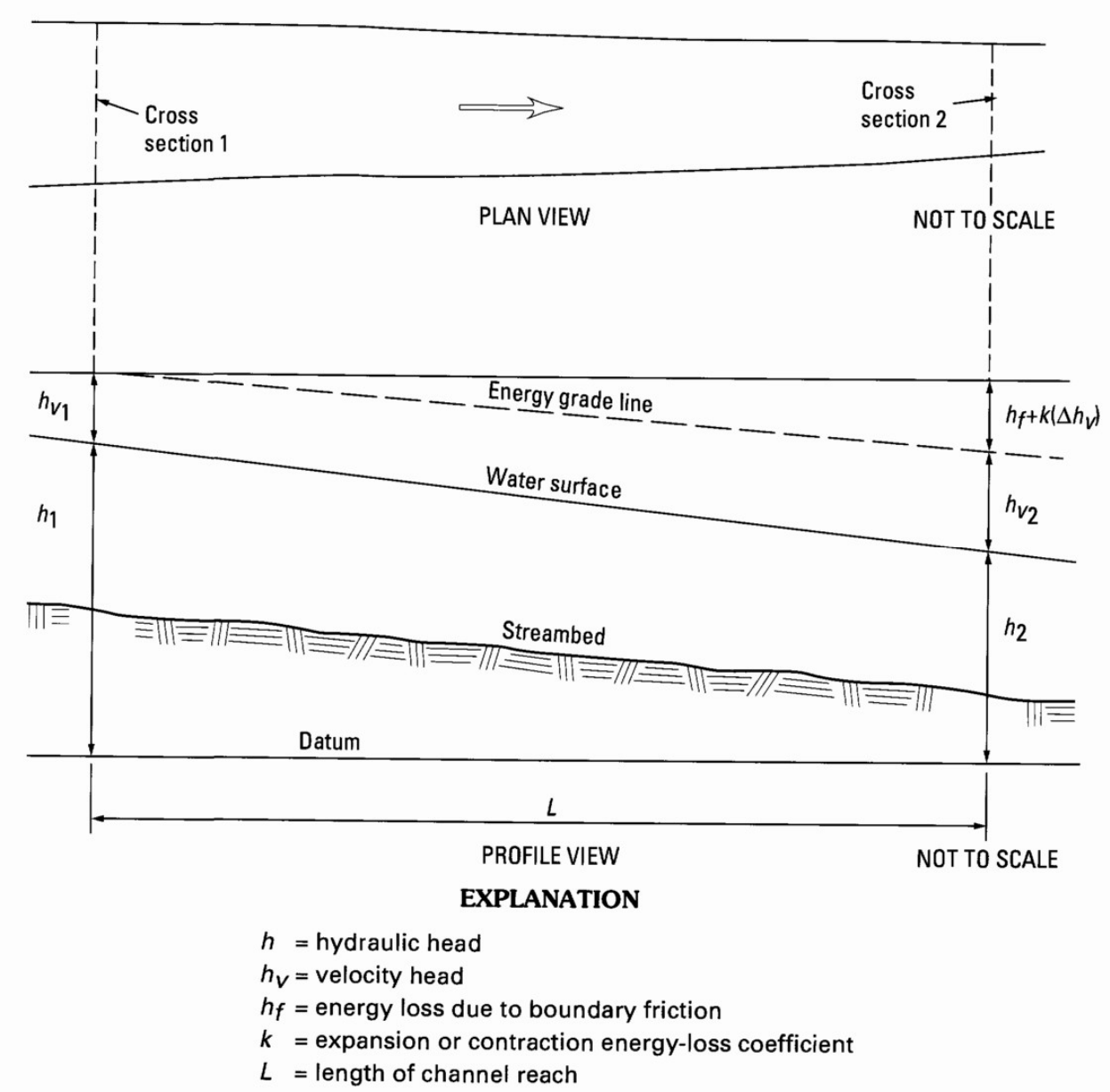

Figure 2. Definition sketch of the analytical solution for n given a multi-section reach (Coon, 1998, p. 12)

3.2 Flow-Retarding Factors

Cowan's visual method requires the knowledge of a base n value and 5 flow retarding factors. The equation that represents Cowan's relationship is as follows:

Equation 15. Equation for Cowan's visual method

$$n = (n_0 + n_1 + n_2 + n_3 + n_4)m$$

Where n_0 is the base value for a straight, uniform channel, n_1 is a value that accounts for the effect of cross section irregularity, n_2 is a value that accounts for the change in size and shape of the channel, n_3 is a value that accounts for the effect of obstructions, n_4 is a value that accounts

for the type and density of vegetation, and m is a value that accounts for the degree of channel meandering (sinuosity). Equation 16 below presents the relationship for determining the sinuosity of a reach, where L_l is the reach's profile length and L_s is the shortest path from the upstream to downstream cross sections. Additionally, Table 1 and Table 2 present the base values used for n_0 and the rest of the factors respectively.

Equation 16. Sinuosity of a channel

$$Sinuosity = \frac{L_l}{L_s}$$

Table 1. Base values for n_0 when using Cowan's method

Type of channel and bed material	Base n value		
	Benson and Dalrymple	Chow	Bray
Sand channels (upper regime flow only)	0.012	-	-
	0.017	-	-
	0.02	-	-
	0.022	-	-
	0.023	-	-
	0.025	-	-
	0.026	-	-
Stable channels			
Concrete	0.012-0.018	0.011	-
Rock cut	-	0.025	-
Firm earth	0.025-0.032	0.02	-
Coarse sand	0.026-0.035	-	-
Fine gravel	-	0.024	-
Gravel	0.028-0.035	-	-
Coarse gravel	-	0.028	-
Very coarse gravel	-	-	0.032
Small cobble	-	-	0.036
Cobble	0.030-0.050	-	-
Boulder	0.040-0.070	-	-

Table 2. Factors for calculating an n value based on Cowan's method (Coon, 1998, pp. 10-11)

[Original source of data presented in this table is Cowan (1956). Modifications from Chow (1959), Aldridge and Garrett (1973), and Jarrett (1985, table 1) are included. Italicized examples of vegetation are based on results of data presented in this report]

Channel condition	*n* value adjustment[1]	Example
Cross-section irregularities, n_1:		
Smooth	0.000	Compares with the smoothest channel attainable in a given bed material.
Minor	0.001–0.005	Compares with carefully dredged channels in good condition but having slightly eroded or scoured side slopes.
Moderate	0.006–0.010	Compares with dredged channels having moderate to considerable bed roughness and moderately sloughed or eroded side slopes.
Severe	0.011–0.020	Badly sloughed or scalloped banks of natural streams; badly eroded or sloughed sides of canals or drainage channels; unshaped, jagged, and irregular surfaces in channels in rock.
Channel variations, n_2: (Do not reevaluate channel variation in the hydraulic computations.)		
Gradual	0.000	Size and shape of channel cross sections change gradually.
Alternating occasionally	0.001–0.005	Large and small cross sections alternate occasionally, or the main flow occasionally shifts from side to side owing to changes in cross-sectional shape.
Alternating frequently	0.010–0.015	Large and small cross sections alternate frequently, or the main flow frequently shifts from side to side owing to changes in cross-sectional shape.
Effect of obstruction, n_3:		
Negligible	0.000–0.004	A few scattered obstructions, which include debris deposits, stumps, exposed roots, logs, piers, or isolated boulders, that occupy less than 5 percent of the cross-sectional area.
Minor	0.005–0.015	Obstructions occupy less than 15 percent of the cross-sectional area, and the spacing between obstructions is such that the sphere of influence around one obstruction does not extend to the sphere of influence around another obstruction. Smaller adjustments are used for curved smooth-surfaced objects than are used for sharp-edged angular objects.
Appreciable	0.020–0.030	Obstructions occupy from 15 to 50 percent of the cross-sectional area, or the space between obstructions is small enough to cause the effects of several obstructions to be additive, thereby blocking an equivalent part of a cross section.
Severe	0.040–0.060	Obstructions occupy more than 50 percent of the cross-sectional area, or the space between obstructions is small enough to cause turbulence across most of the cross section.
Channel vegetation,[2] n_4:		
Negligible	0.000	*Any type or density of vegetation growing on the banks of channels more than about 100 ft wide with less than 25 percent of the wetted perimeter vegetated and no significant vegetation along channel bottoms. Mowed grass or vetch on banks of channels over 50 ft wide. (Could be applicable to narrower channels.)*
Small	0.002–0.010	Dense growths of flexible turf grass, such as Bermuda, or weeds growing where the average depth of flow is at least two times the height of the vegetation; supple tree seedlings such as willow, cottonwood, arrowweed, or saltcedar growing where the average depth of flow is at least three times the height of the vegetation. *Dense, woody brush, annual soft-stemmed plants, and possibly a few mature trees that cover 25 to 50 percent of the wetted perimeter in any season on the banks of channels 100 to about 250 ft wide and during the dormant season on the banks of channels 30 to about 100 ft wide.*
Channel vegetation,[2] n_4—Continued:		
Medium	0.010–0.025	Turf grass growing where the average depth of flow is from one or two times the height of the vegetation; moderately dense stemmy grass, weeds, or tree seedlings growing where the average depth of flow is from two to three times the height of the vegetation; brushy, moderately dense vegetation, similar to 1- to 2-year-old willow trees in the dormant season, *or tall grasses and soft-stemmed plants in the growing season*, growing along the banks and no significant vegetation along the channel bottoms where the hydraulic radius exceeds 2 ft. *Dense, woody brush, annual soft-stemmed plants, and possibly a few mature trees that cover 25 to 50 percent of the wetted perimeter on the banks of channels 30 to about 100 ft wide during the growing season.*
Large	0.025–0.050	Turf grass growing where the average depth of flow is about equal to the height of vegetation; 8- to 10-year-old willow or cottonwood trees intergrown with some weeds and brush (none of the vegetation in foliage) where the hydraulic radius exceeds 2 ft; bushy willows about 1 year old intergrown with some weeds along side slopes (all vegetation in full foliage) and no significant vegetation along channel bottoms where the hydraulic radius is greater than 2 ft.
Very large	0.050–0.100	Turf grass growing where the average depth of flow is less than half the height of the vegetation; bushy willow trees about 1 year old intergrown with weeds along side slopes (all vegetation in full foliage) or dense cattails growing along channel bottom; trees intergrown with weeds and brush (all vegetation in full foliage).
Degree of meandering, m[3,4]:		
Minor	1.00	Ratio of the channel meander length (L_m) to valley or straight-channel length (L_s) is 1.0 to 1.2.
Appreciable	1.15	L_m/L_s is 1.2 to 1.5.
Severe	1.30	L_m/L_s is greater than 1.5.

[1]Adjustments are based primarily on data from channels less than 60 ft wide and are probably applicable for channels as much as 100 ft wide, unless otherwise specified. Larger adjustments generally are necessary for narrower channels.

[2]Note the distinction in the examples between vegetation distributed uniformly across a channel, which is assumed, and bank vegetation alone.

[3]Adjustment values apply to flow confined in the channel and do not apply where downvalley flow crosses meanders.

[4]Adjustments for cross-section irregularities, channel variations, effect of obstructions, and channel vegetation are added to the initial *n* value (tables 1, 2, or 3 or the estimation equations). This sum is multiplied by the adjustment factor for degree of meandering.

3.3 Site Conditions

The site chosen for this study was from a subwatershed, called the South Fork, that is a part of the larger Chester Creek Watershed in South Central Alaska. The upper drainage basin of the South Fork is the main headwaters for the watershed and originates in the Chugach Mountains. It then feeds into the lower drainage basin in the Anchorage Bowl and drains into the manmade gravel extraction of University Lake. It is worth noting that the Lower South Fork is the largest drainage basin in the watershed at about 6,265 acres, while the size of University Lake is 21.1 acres (Anchorage Waterways Council, 2014).

The creek then feeds into the study area, a small basin bounded by Mallard Lane, UAA Drive, Providence Drive, Spirit Drive, Spirit Way, and Seawolf Drive. This basin is about 18.5 acres. Figure 3 shows the location of the entire Chester Creek Watershed in relation to Alaska. Moreover, the bottom figure shows the project area circled in red. Figure 4 then provides a closer look of this red circle in order to present the project site in more detail. It can be seen in Figure 4 that there are two tributaries connected to the main reach. These tributaries are small, dredged drainage channels. The upstream tributary origin is the outlet of a culvert that runs under UAA Drive. The downstream tributary is also a drainage outlet, originating from a culvert that exits the NW parking lot of UAA. Due to limitations on time, these tributaries were not included in the analysis for this project.

Data was collected from the site during March. Therefore, about 2 feet of snow was present on the top banks and flood plains. This meant that the vegetation makeup of the floodplain could not be identified. Flow inside the channel was deeper and quicker than usual due to spring runoff conditions. The representative reach itself was about 980 feet long and consisted of 17 cross sections. Figure 5 shows the representative reach and the location of the surveyed cross sections. The bed makeup was not recorded for the channel. However, a considerable amount of time was spent walking on the channel bed during data collection. It was observed that the bed make up felt like a larger material, with very large boulders also being frequent. Additionally, a considerable amount of obstructions were present in the form of downed trees. The water in the channel appeared clear and there was little to no growing vegetation present on the channel bed. Furthermore, the basin resides in a heavily wooded area with a pedestrian path cutting through it. The pedestrian path contains a small wooden bridge that permits foot traffic over the channel.

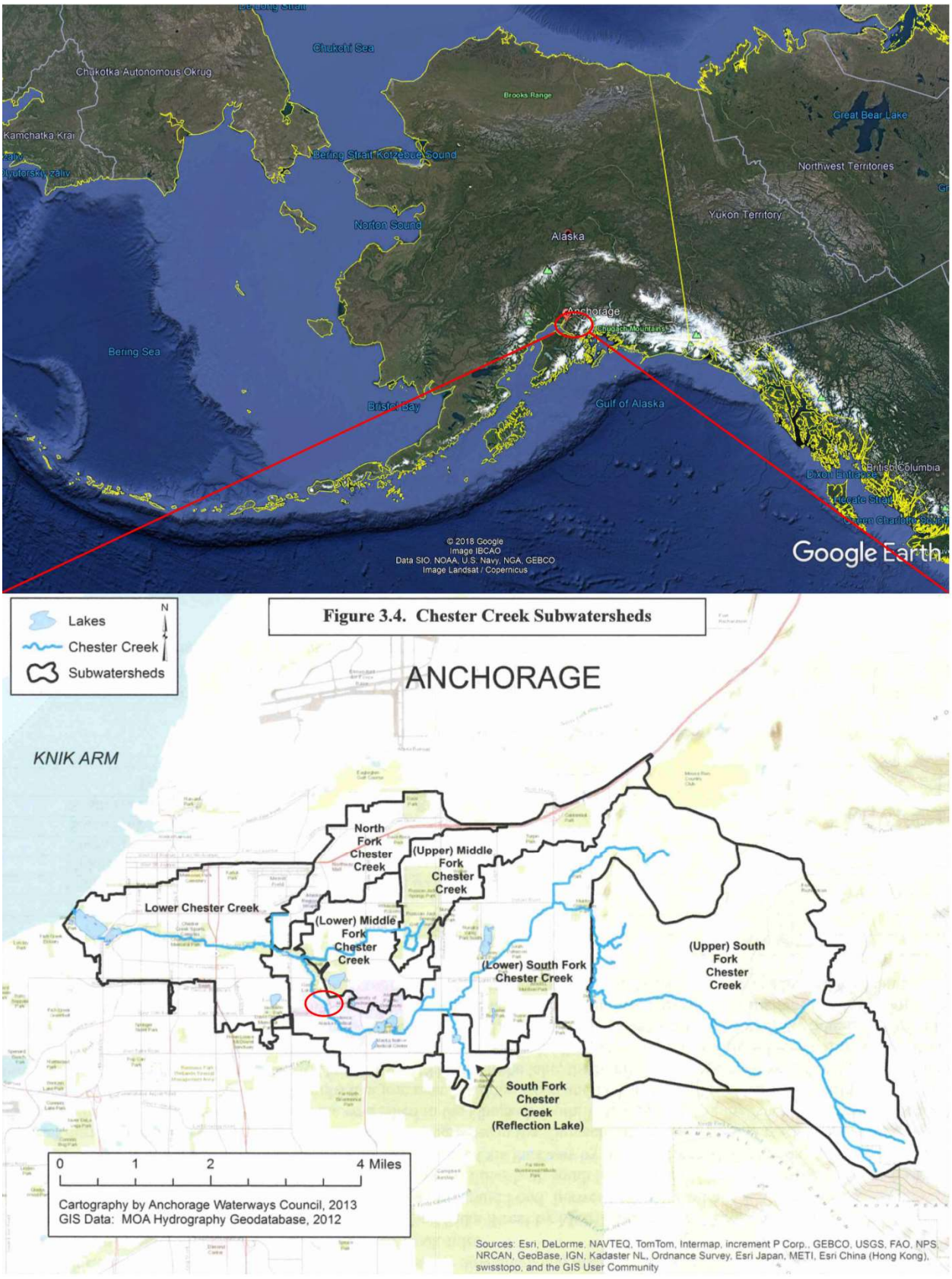

Figure 3. Top: Alaska; Bottom: Chester Creek Watershed (Anchorage Waterways Council, 2014) with project site circled in red

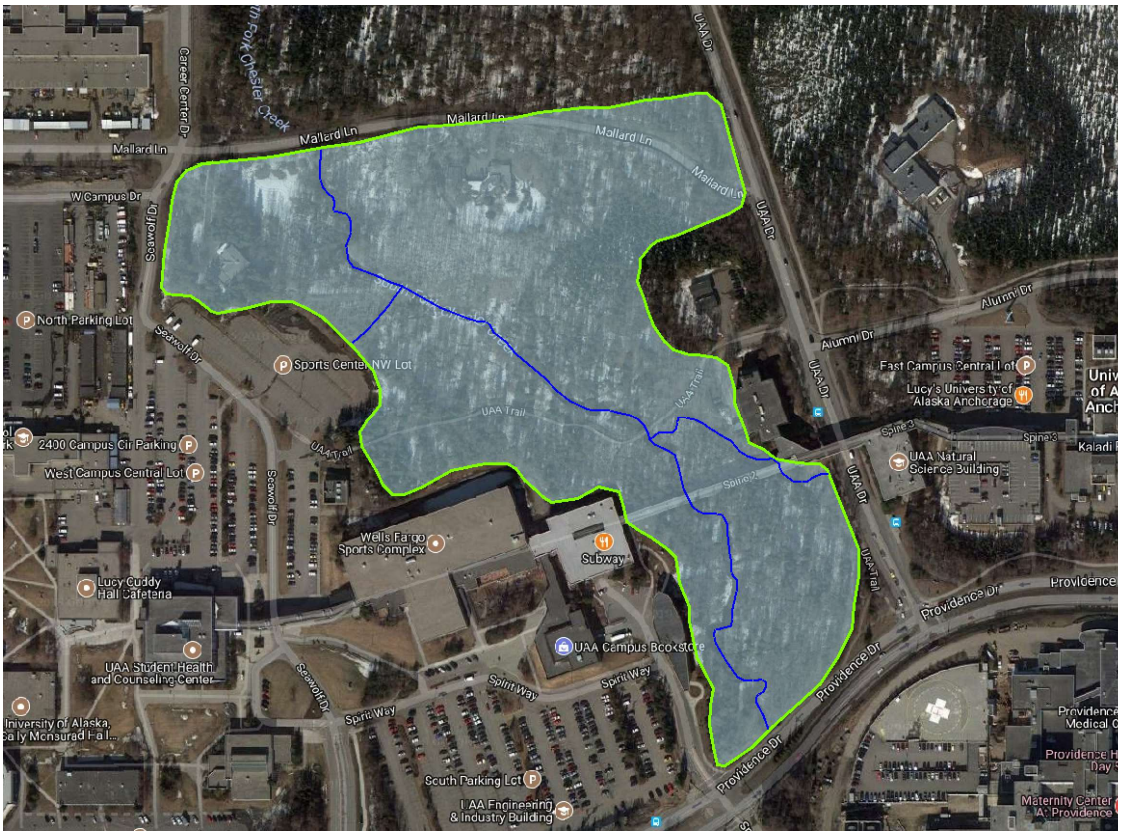

Figure 4. Project site drainage basin

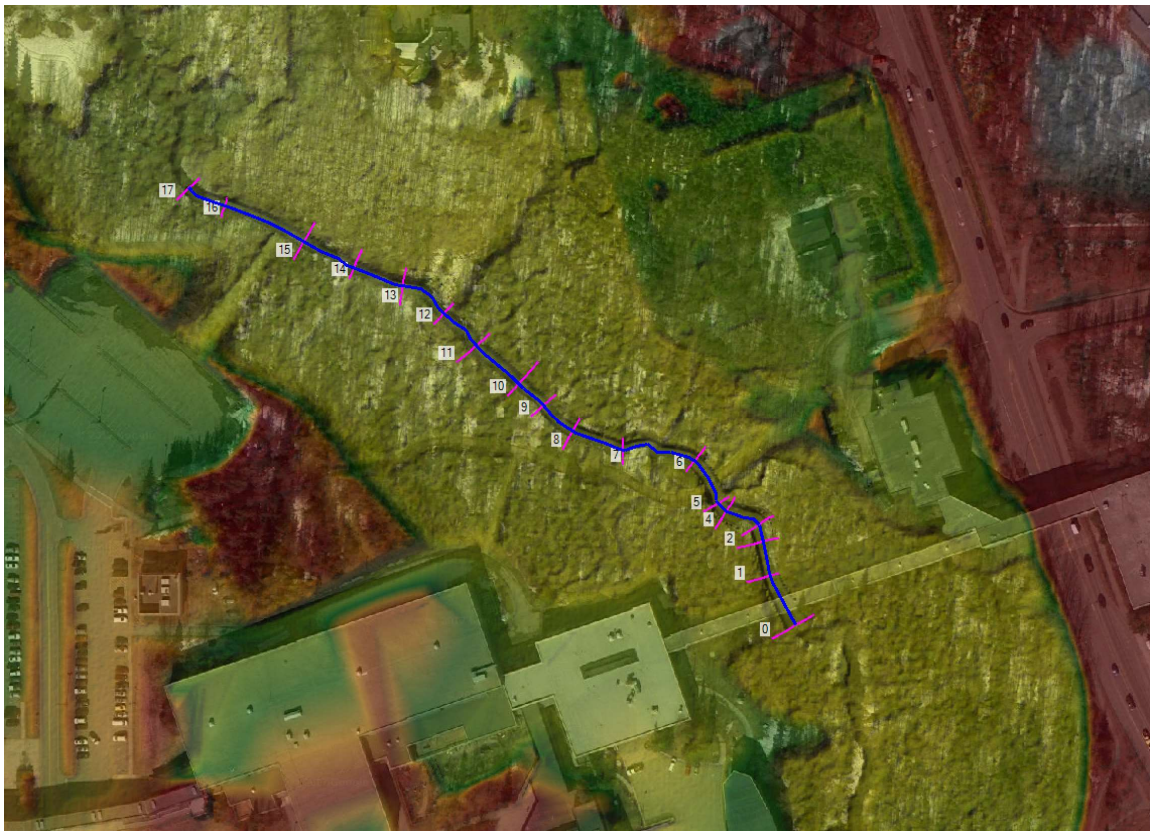

Figure 5. Representative reach and its cross section locations

3.4 Data Collection and Model Generation

Data collection consisted of a basic survey using NAVD88 (North American Vertical Datum of 1988) GPS orthometric elevations. The GPS and controller used was a Leica GS14 and GS15 respectively. Elevations were adjusted to the MOA72 datum by adjusting original recorded elevations by -6.29 feet. As stated before, the survey consisted of a 980-foot profile and 17 cross sections and can be seen in Figure 5. Cross section locations were chosen on the basis of creating an accurate representation of the reach.

In order to create the channel profile in HEC-RAS and properly reference the GPS points recorded in the field, a terrain model had to be created in the RAS Mapper tool of HEC-RAS. The Municipality of Anchorage has an online database of downloadable Lidar tiles at https://muniorg.maps.arcgis.com/apps/webappviewer/index.html?id=fc1b55ac4abe44769ee2daef94217bce. For the project, the photo TIF file on the MOA72 datum was downloaded for the 1668_2626 tile. With the terrain downloaded, the file was imported into RAS Mapper and the projection associated with the TIF file was set automatically by the program.

When a terrain is created in RAS Mapper, the Easting and Northing coordinates can be seen in the HEC-RAS Geometry Editor due to the projection. More specifically, as a user moves their curser around the terrain model, the coordinates of the curser will be displayed in the bottom right corner. With the GPS coordinates of the profile points also being in Easting and Northing, an accurate profile can be created in the model that is the same as the observed field conditions. This was done manually by moving the cursor to each given coordinate and creating a profile point at said location. The cross section points were also given in Easting and Northing coordinates. The center point of the cross section was taken as the location of the cross section on the profile. All cross section data was then entered manually in the cross section tab of the geometry editor. Figure 5 shows the final profile of the reach as well as the location of each cross section on the profile. Figure 5 also includes the terrain superimposed on top of a satellite image.

Although Figure 5 represents an accurate representation of field conditions, it is only useful for display purposes in this case. Normally, a model like Figure 5 would be perfectly valid when running simulations in HEC-RAS. However, for reasons explained in the next section, a model like Figure 5 does not aid in the analysis for this project. Therefore, a second model that depends on observed flow conditions was created for the analytic method.

The flow conditions that were needed for the analytic method consisted of water depth and flow velocity at each cross section. The water depth was measured with a standard tape measure at the deepest point of the surveyed cross section. Given the elevation of the deepest point from the survey data and the recorded water depth at said point, the WSE elevation was calculated by adding the two together. As for the flow, the velocity at each cross section was recorded with an electromagnetic flowmeter while wading in the creek. The meter used was a Marsh-McBirney Flo-Mate Model 2000 Portable Flowmeter in conjunction with a Rickly USGS Top Setting Wading Rod. Both devices can be seen in Figure 6. It is worth noting that this flowmeter has an accuracy tolerance of 2%. Readings were taken every 6 inches using the 0.6 depth method (Herschy, 2009, p. 21). It should be noted that the average velocity depth location is estimated by the wading rod. The flow readings across the cross section were then averaged into a single representative value for each cross section.

Figure 6. Marsh-McBirney Flo-Mate Model 200 Portable Flowmeter and Rickly USGS Top Setting Wading Rod

3.5 Method Applications

Analytic Method

The analytic method requires the use of Equation 14. It can be seen from Equation 14 that the flow rate, head loss, reach length, cross sectional area, and cross sectional hydraulic radius must be known. Equation 14 also shows that some of these variables are needed at every cross section in order to properly weight the final roughness coefficient. More specifically, the part of the head loss term that accounts for head loss due to changes in acceleration requires the change in velocity head from cross section to cross section. Additionally, the length from one cross section to the next is weighted with the Z term of both cross sections. Moreover, the value of Z ($AR^{2/3}$)

depends on the WSE because it is based on the wetted area and perimeter of the channel. In summation, a velocity and water depth are required at each cross section to use Equation 14. The more difficult part of this is calculating the wetted area and perimeter for Z. This is because the cross sections are not generic shapes, so there are no explicit equations to calculate their hydraulic properties. Numerical integration must be used across their width in order to find their wetted area and perimeter. This is where HEC-RAS comes in.

Part of the HEC-RAS output during simulations are the hydraulic properties for each cross section. Therefore, it can be used to create a model that will output the variables needed for Equation 14. In a similar fashion to the previously presented calibration method, a model of 17 sperate reaches was created for each of the 17 cross sections. This was done because the hydraulic properties of each individual cross section were needed, not the nature of the entire channel as a whole. The boundary condition used for each reach were the known WSE's, which can be seen in Figure 7. This was used so that the correct hydraulic properties would be output based on the observed WSE. HEC-RAS also requires a manning roughness and flowrate input to run a simulation. Due to the fact that this simulation was run purely on the basis of finding the wetted area and perimeter, the provided flow and roughness became arbitrary. As long as the correct WSE was achieved in the model, the correct A and P could be recorded. A sample output for a cross section has been include in Figure 8, while Figure 9 includes a graphical output of the observed conditions.

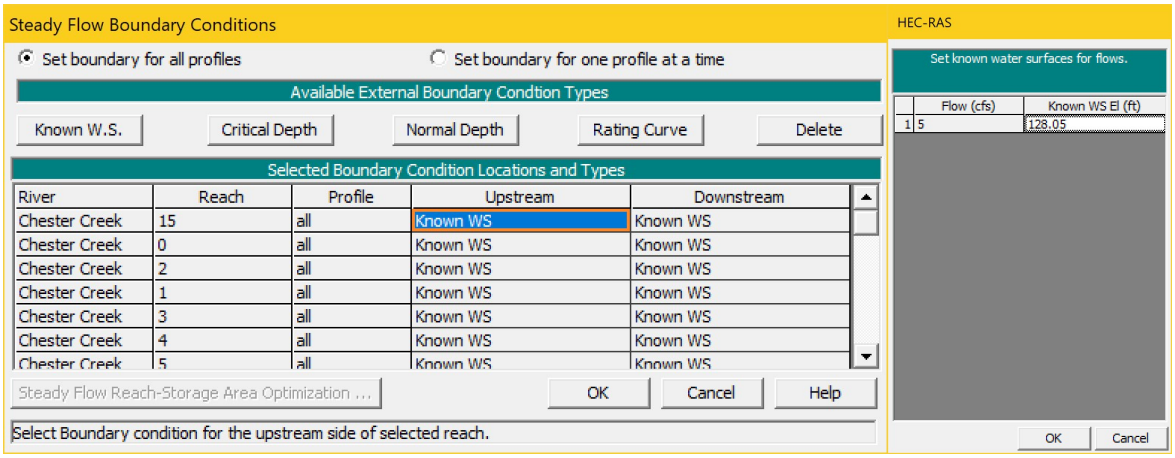

Figure 7. Setting boundary conditions for HEC-RAS model

Cross Section Output

File Type Options Help

River: Chester Creek Profile: PF 1

Reach 15 RS: 0 Plan: A and P Calc

Plan: A and P Calc Chester Creek 15 RS: 0 Profile: PF 1

		Element	Left OB	Channel	Right OB
E.G. Elev (ft)	128.05	Wt. n-Val.		0.095	
Vel Head (ft)	0.00	Reach Len. (ft)			
W.S. Elev (ft)	128.05	Flow Area (sq ft)		23.61	
Crit W.S. (ft)	126.93	Area (sq ft)		23.61	
E.G. Slope (ft/ft)	0.001028	Flow (cfs)		12.86	
Q Total (cfs)	12.86	Top Width (ft)		20.27	
Top Width (ft)	20.27	Avg. Vel. (ft/s)		0.54	
Vel Total (ft/s)	0.54	Hydr. Depth (ft)		1.17	
Max Chl Dpth (ft)	1.59	Conv. (cfs)		401.0	
Conv. Total (cfs)	401.0	Wetted Per. (ft)		20.87	
Length Wtd. (ft)		Shear (lb/sq ft)		0.07	
Min Ch El (ft)	126.46	Stream Power (lb/ft s)		0.04	
Alpha	1.00	Cum Volume (acre-ft)			
Frctn Loss (ft)		Cum SA (acres)			
C & E Loss (ft)					

Errors, Warnings and Notes

Select Profile

Figure 8. Sample output for cross section 15

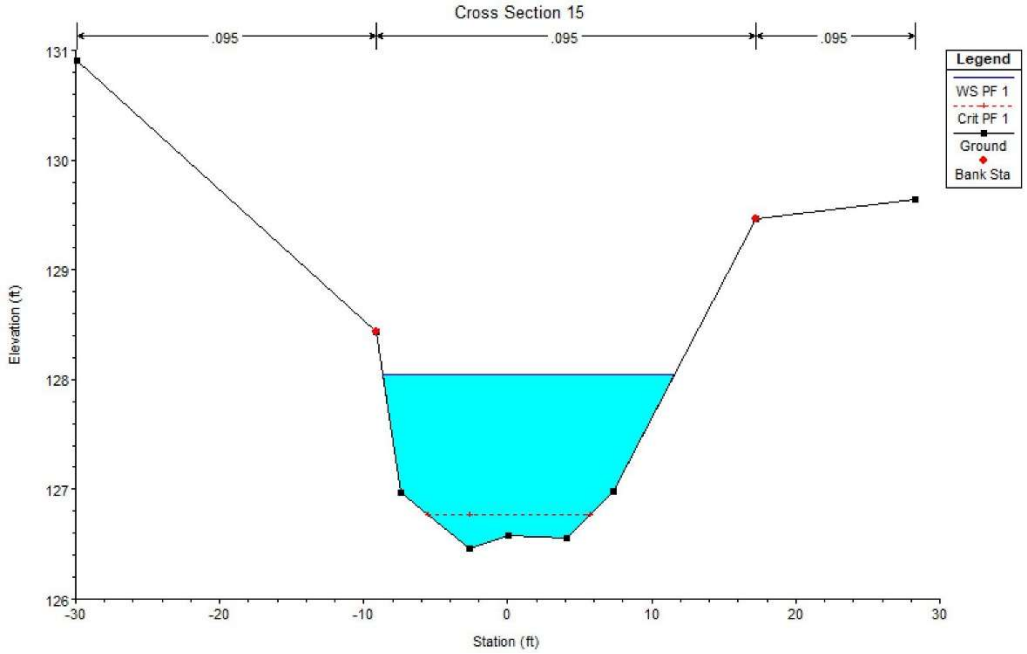

Figure 9. Sample graphical output of observed conditions simulation in HEC-RAS

An additional variable not yet discussed is the expansion/contraction coefficient, k. As stated previously, it is used in the head loss calculation to account for losses due to accelerations or decelerations when reaches expand or contract. It is worth noting that this requires the knowledge of the entire area of the cross section. This information was obtained in HEC-RAS with a similar technique to the one described previously. The difference here is that the WSE boundary condition was set to the max bank elevation of the cross section. Therefore, HEC-RAS outputs the bank full wetted area of the cross section, which in this case is entire cross sectional area. With the known areas from the HEC-RAS model, a value for k was quickly determined based on the difference in area from cross section to cross section. An increase in area constitutes expansion and a k value of 0.5, while a decrease in area constitutes contraction and a k value of 0.

The last variable unaccounted for is the flow rate, Q. With known velocities and areas at each cross section, a subsequent Q was calculated using the continuity equation described in Equation 13. To confirm this is valid, a quick check in HEC-RAS was done. Looking at cross section 15 in Table 4, it can be seen that the calculated flow from the recorded velocity and area was 12.86 cfs. Putting that flow as an input into the HEC-RAS model should output the same recorded velocity of 0.54 ft/s. Figure 8 shows just that. On the left side of the output for cross section 15, it can be seen that the Q total is equal to 12.86 cfs, while the right side of the output gives an average velocity of 0.54 ft/s. Additionally, both flow areas and WSE's remained the same. With the Q value confirmed, a weighted value for Q was then calculated using the following relationship:

Equation 17. Weighted flow rate for a multi-section channel

$$Q = \frac{Q_1 Z_1 + Q_2 Z_2 + \cdots + Q_m Z_m}{Z_1 + Z_2 + \cdots + Z_m}$$

Where Z, as defined before, is $AR^{2/3}$. A weighted value for the flow rate was used instead of an average because of the changing cross section geometries. With the flow rate's dependence on cross section geometry, an average value would not be an accurate representation of observed conditions.

With the weighted flow rate, mean velocity and WSE readings at each cross section from field observations, the distance between cross sections from the survey, and wetted area and perimeter

of each cross section from the HEC-RAS model, Equation 14 could finally be used. Table 3 and 4 present all the data used in Equation 14 to calculate the final weighted n value for the reach.

Table 3. Hydraulic properties of each cross section from HEC-RAS model

Station	Depth (ft)	Bottom Point Elevation (ft)	WSE (ft)	A (ft^2)	P (ft)	R (ft)	L (ft)	Max Bank Elevation (ft)	Total A (ft^2)	ΔA (%)	k
15	1.08	126.97	128.05	23.61	20.87	1.13	-	129.46	56.67	-	-
14	0.42	125.89	126.31	5.05	17.09	0.30	66.63	128.93	53.93	-0.05	0
13	0.75	125.67	126.42	14.75	18.72	0.79	41.83	128.73	62.18	0.15	0.5
12	0.96	124.85	125.81	16.20	23.01	0.70	20.48	128.60	86.63	0.39	0.5
11	1.03	125.03	126.06	27.88	21.17	1.32	43.61	128.52	83.62	-0.03	0
10.5	0.91	124.58	125.49	9.08	13.66	0.66	13.82	127.49	39.15	-0.53	0
10	0.29	124.67	124.96	9.21	15.75	0.58	59.73	127.53	53.77	0.37	0.5
9	0.90	123.74	124.64	22.88	18.54	1.23	91.76	126.07	49.98	-0.07	0
8	0.75	123.07	123.82	13.70	16.15	0.85	64.48	125.55	41.94	-0.16	0
7	0.75	122.20	122.95	7.28	11.32	0.64	47.53	124.75	32.38	-0.23	0
6	0.51	122.60	123.11	15.12	13.20	1.15	39.34	124.72	38.65	0.19	0.5
5	1.09	120.49	121.58	12.78	13.95	0.92	68.55	123.86	52.93	0.37	0.5
4	0.82	120.77	121.59	11.75	12.17	0.97	55.18	123.61	38.92	-0.26	0
3	0.29	120.02	120.31	6.01	11.48	0.52	62.55	124.25	68.16	0.75	0.5
2	0.89	119.79	120.68	20.35	15.10	1.35	62.59	122.18	44.69	-0.34	0
1	0.49	118.77	119.26	5.67	11.15	0.51	67.57	121.41	37.21	-0.17	0
0	0.51	118.44	118.95	14.55	13.40	1.09	58.93	120.99	47.69	0.28	0.5

Table 4. Flow rates and head losses at each cross section based on observed velocity readings

Station	Average Flow Velocity Over Cross Section (m/s)	v (ft/s)	A (ft^2)	Q (ft^3/s)	α	g (ft/s^2)	h_v (ft)	Δh_v (ft)
15	0.17	0.54	23.61	12.86	1	32.174	0.005	
14	0.89	2.91	5.05	14.68	1	32.174	0.131	-0.127
13	0.30	1.00	14.75	14.71	1	32.174	0.015	0.116
12	0.45	1.49	16.20	24.13	1	32.174	0.034	-0.019
11	0.22	0.71	27.88	19.76	1	32.174	0.008	0.027
10.5	0.60	1.98	9.08	17.99	1	32.174	0.061	-0.053
10	0.47	1.54	9.21	14.20	1	32.174	0.037	0.024
9	0.39	1.29	22.88	29.58	1	32.174	0.026	0.011
8	0.63	2.07	13.70	28.41	1	32.174	0.067	-0.041
7	0.56	1.84	7.28	13.38	1	32.174	0.052	0.014
6	0.22	0.71	15.12	10.71	1	32.174	0.008	0.045
5	0.55	1.80	12.78	22.98	1	32.174	0.050	-0.042
4	0.54	1.78	11.75	20.97	1	32.174	0.050	0.001
3	0.45	1.47	6.01	8.83	1	32.174	0.034	0.016
2	0.33	1.10	20.35	22.30	1	32.174	0.019	0.015
1	0.36	1.18	5.67	6.70	1	32.174	0.022	-0.003
0	0.31	1.00	14.55	14.61	1	32.174	0.016	0.006

If a more detailed look at the observed conditions for each cross section is desired, refer to Section 2 of the Appendix. It contains the most important observed conditions, site photographs, and a HEC-RAS graphical output for each cross section.

Visual Method

Cowan's visual method is represented in Equation 15 and uses values based on Equation 16, Table 1, and Table 2. Using the data provided for the profile points from the survey, the total length and shortest path of the channel was calculated in order to find the sinuosity of the

channel from Equation 16. Then, based on visual observations, each coefficient from Equation 15 was assigned an approximate representative value from Table 1 and 2. After all the coefficients in Equation 16 were assigned, the approximate Manning's n value for the channel was calculated using said equation.

Empirical Method

Sauer's method in Equation 9 was chosen as the empirical method for this study because its relationship relies on both the water surface slope and the hydraulic radius. S_w from Equation 9 was calculated by dividing the change in WSE by the distance between two cross sections. The data required for this was already recorded in Table 3, as well as the hydraulic radius. With these two values, Equation 9 was implemented at each cross section to produce a roughness coefficient for each location. In a similar manner to Equation 17, Equation 18 then weighted the Manning roughness value for a final empirical composite coefficient for the reach.

Equation 18. Weighted Manning roughness for a multi-section channel using Sauer's empirical relationship

$$n = \frac{n_1 Z_1 + n_2 Z_2 + \cdots + n_m Z_m}{Z_1 + Z_2 + \cdots + Z_m}$$

4.0 Results

4.1 Numerical Output

A Manning roughness of 0.0706 was found for the analytical method, which can be seen in Table 5. Cowan's visual method produced a somewhat similar result of 0.077, which can be seen in Table 6. Sauer's empirical relationship produced the most surprising result at 0.045, which can be seen in Table 7.

Table 5. Results for the analytical method

h_{15} (ft)	128.05
h_0 (ft)	118.95
h_{v15} (ft)	0.005
h_{v0} (ft)	0.016
$\Sigma(k*\Delta h_v)$	0.073
$\Sigma(L/Z^2)$	10.76
Q (ft^3/s)	19.26
n	0.071

Table 6. Results for Cowan's visual method

n_b	0.03
n_1	0.008
n_2	0.005
n_3	0.025
n_4	0.002
m	1.1
n	0.077

Table 7. Results for Sauer's empirical relationship

Σ (n*Z)	9.233
Σ (Z)	206.32
n_w	0.0447

4.2 Analysis

It was found that the analytical method and visual method produced similar results, while the empirical relationship was quite different. According to Chow's table of roughness coefficients (Section 1 of the Appendix), the project site falls under the minor natural stream designation. Furthermore, due to the large amount of obstructions in the stream and ineffective flow areas (many deep, calm pools present on the outer edges of turns), the project reach would fall under

description 8, “Very weedy reaches, deep pools, or floodways with heavy stand of timber and underbrush.” Therefore, Chow’s table predicts a Manning roughness from 0.075 to 0.150. Even though the analytical method does not fall in this range, the minimum of the range is much closer to the analytical and visual values compared with the empirical value. Additionally, using Hicks and Mason’s book, the project reach is most closely related to site 37503 (Hicks & Mason, 1998, pp. 278-281). This comparison can be seen in Table 8. Hicks and Mason’s results seem to agree with Chow’s table given that their value for n was 0.11, which falls within Chow’s range.

Table 8. A comparison of project site values with Hicks and Mason's values from "Roughness Characteristics of New Zealand Rivers”

Variable	Project Value	Book Value
Q (m^3/s)	0.55	0.49
S_f	0.0092	0.0094
WSS	0.0093	0.0095
n	0.071	0.11

It is important to note that there are a few limitations that come with using Sauer’s empirical relationship. The equation is only applicable for water surface slopes between 0.0003 and 0.018. Table 9 shows that the data used for the calculation violates these stipulations in all but 4 locations. However, an additional calculation with only the valid cross sections still produces a value of 0.044.

Table 9. Data used for Sauer's empirical relationship

WSE (ft)	L (ft)	S_w (ft/ft)	R (ft)	n	Z	n*z
128.05	-	-	1.13	-	25.63	-
126.31	66.63	0.0262	0.30	0.0518	2.24	0.116
126.42	41.83	-0.0027	0.79	0.0372	12.58	0.469
125.81	20.48	0.0299	0.70	0.0569	12.82	0.729
126.06	43.61	-0.0058	1.32	0.0445	33.50	1.491
125.49	13.82	0.0416	0.66	0.0601	6.92	0.415
124.96	59.73	0.0088	0.58	0.0449	6.44	0.289
124.64	91.76	0.0036	1.23	0.0405	26.32	1.067
123.82	64.48	0.0127	0.85	0.0494	12.28	0.607
122.95	47.53	0.0183	0.64	0.0517	5.42	0.280
123.11	39.34	-0.0041	1.15	0.0413	16.55	0.684
121.58	68.55	0.0223	0.92	0.0551	12.06	0.664
121.59	55.18	-0.0002	0.97	0.0229	11.48	0.263
120.31	62.55	0.0205	0.52	0.0519	3.90	0.203
120.68	62.59	-0.0058	1.35	0.0446	24.83	1.107
119.26	67.57	0.0210	0.51	0.0520	3.61	0.188
118.95	58.93	0.0052	1.09	0.0430	15.37	0.661

5.0 Conclusions

5.1 Discussion

From the results in the previous section, it can be concluded that the analytical and visual methods used are valid for this project site. The visual method produces a value that falls within Chow's table, while the analytical method falls within 5% of Chow's table. Additionally, a similar reach studied in Hicks and Mason's book produces a value that falls within Chow's table (Hicks & Mason, 1998, pp. 278-281). It can also be concluded that the empirical method is not valid for this project site. Sauer's empirical relationship produces a value well below the trend of the other results. In fact, it is about 40% from the values that Chow's table gives.

In summation, the Manning roughness coefficient produced by the analytical method, 0.071, is recommended for this reach. Even though this method produced a value outside of Chow's recommended range, it is still within 5% of said range. Additionally, it is the exact solution of the observed conditions instead of being an estimation. Furthermore, the minimum value governs for Manning roughness coefficients because of the Manning equation. A smaller n causes a larger flow. In that sense, a value of 0.071 is the least of the two valid answers. It is worth noting that this discrepancy in answers highlights the need for using multiple methods. It is recommended no one estimation method be used while assigning an n value. However, as previously presented, many different methods exist. Project limitations should govern which methods are chosen for a roughness analysis.

5.2 Possible Sources of Error

The uncertainties in the calculated values of Manning's n are due to measurement error. More specifically, most of the time, the 95% confidence level uncertainties in the calculated roughness coefficients are governed by the measurement errors associated with the discharge. In this case, the discharge values are the velocity measurements. The root-sum-square method was used to calculate the error propagation, provided by Equation 19 (Herschy, 2009, p. 456).

Equation 19. Error propagation for measuring discharge

$$u(Q) = \left[{u_m}^2 + {u_s}^2 + \left(\frac{1}{m}\right)\left({u_b}^2 + {u_d}^2 + {u_p}^2 + \left(\frac{1}{n}\right)\left({u_c}^2 + {u_e}^2 \right) \right) \right]^{1/2}$$

Where u_m is the uncertainty due to limited number of verticals (i.e. the number of measurements taken across the channel), u_s is the uncertainty, or rating, of the current meter, u_b is the uncertainty due to the width of the channel, u_d is the uncertainty in the depth measurement, u_p is the uncertainty due to the number of measurements taken per vertical, u_c is the uncertainty in the current meter rating, u_e is the uncertainty due to limited measurement exposure time, m is the number of verticals used in the measurement, and n is the number of points used per vertical in the measurement. Each of these coefficients can be found using the tables provided by Herschy (Herschy, 2009, pp. 463-465). For instance, Table 10 shows Herschy's table for calculating u_e.

Table 10. A table from Herschy's book, "Streamflow Measurement" for assigning u_e when calculating the uncertainty in measured discharge (Herschy, 2009, p. 464)

Table 13.5 Percentage uncertainties in point velocity measurements due to limited exposure time, u_e

Velocity m/s	Point in vertical							
	0.2D, 0.4D or 0.6D				0.8D or 0.9D			
	Exposure time min							
	0,5	1	2	3	0,5	1	2	3
0.050	25	20	15	10	40	30	25	20
0.100	14	11	8	7	17	14	10	8
0.200	8	6	5	4	9	7	5	4
0.300	5	4	3	3	5	4	3	3
0.400	4	3	3	3	4	3	3	3
0.500	4	3	3	2	4	3	3	2
1.000	4	3	3	2	4	3	3	2
over 1.000	4	3	3	2	4	3	3	2

Upon inspection, the uncertainty at cross section 15 governs due the difficulty in measuring the discharge for it. It was observed that the cross section was very calm, to the point that it was almost an ineffective flow area (i.e. a pool). This was due to an impedance in flow immediately upstream and downstream of the cross section. The impedance was the result of a small, natural rock dam downstream and a large area of downed trees and brush upstream. Additionally, the cross section contained several eddies that caused negative velocity readings in several sections.

Therefore, only 5 readings were taken across the width of the cross section. Table 11 shows the subsequent calculation of the governing measurement error.

Table 11. Final propagation in error for the calculated Manning's n

Given	
# of Verticals	5
Points in Vertical	1
Average Velocity (m/s)	0.17
Exposure Time (min)	1
Current Meter Rating	2

u_m	7.5
u_s	2
u_b	0.15
u_d	0.65
u_p	7.5
u_c	1.2
u_e	7.7
u(Q)	9.15

Consequently, the analytical method produced a roughness coefficient of 0.071 ± 9.15%. This error lies within the typical range for discharge measurement errors, which is ± 8% to ± 12% (Hicks & Mason, 1998). Coincidentally, adding the error to the final value produces a value of 0.077, the exact value obtained for the visual method that also falls in the range given by Chow's table.

Uncertainties associated with the survey could have also played a role in error propagation during calculations. However, the survey was performed by a professionally licensed surveyor. Additionally, the equipment used for the survey is far more accurate than the instruments used for the discharge measurements. In this regard, as previously stated, the discharge measurements usually govern the error propagation when conducting hydraulic studies. It is also worth noting that the error in stage measurement is contained within the error propagation calculation for discharge.

Another possible source of error occurs within Cowan's visual method. The method itself has inherent uncertainties because it is based on visual estimation. It is by no means an exact method. For instance, without taking samples, it is hard to know just how "weedy" the bottom of a reach is. Additionally, this study was conducted with no previous experience. A bulk of the visual method relies on experience due to its estimating nature. Without experience, it is difficult to assign accurate values based on Cowan's and Chow's tables. A good example of this is determining the effect of obstructions, coefficient n_3, for Cowan's method. Table 2 shows that an estimation of the percentage of area blocked is needed for this. This estimation is very difficult to make without previously experiencing what other reaches look like.

Given these uncertainties, it is perfectly plausible that the empirical method is valid at face value. However, even the lower bound of the analytical method, 0.065, is too far from the empirical method. With this in mind, and the previously discussed limitations for the method, it is still within reason to conclude that the empirical method is just not applicable in this situation. Regardless, that is not to say the relationship is not valid at all. Given the right circumstances, it may produce an accurate value. In this, it is proven once again that no one method, besides the analytical one, should be used over another. The analytical method is technically an exact value, so its use is recommended above all else. Nonetheless, each project presents its own challenges. The analytical method is tedious and requires a lot of time and data, which may be limited by certain projects. These limitations should govern which method is chosen for a calculation.

Lastly, this project has shown that final values can vary greatly. Therefore, it is recommended that at least two different methods be used so that a comparison can be made. The high uncertainties are just part of water resources. These systems are highly irregular and dynamic, making calculations difficult. Trusting a single calculation at face value, in any engineering field for that matter, is not recommended.

6.0 Recommendations

6.1 Gathering More Data to Perform a Calibration

Due to time constraints, the initial scope of the project could not be fulfilled. Performing the calibration method discussed in the literature review was one of the main goals of the project. This required a lot more data that was not taken. More specifically, a rating curve was required at each cross section. This meant that flow data should have been taken for at least one year for each cross section. It is recommended that this method be implemented in the future to further compare values. This would include calibrating a Manning's n in HEC-RAS for each cross section, and then producing a properly weighted value for the entire reach. Moreover, a relationship for varying n's could be created in the same fashion as Hicks and Mason's book, *Roughness Characteristics of New Zealand Rivers* (Hicks & Mason, 1998). The Manning roughness varies with flow, so developing relationships for n with respect to flow could be very useful for the Municipality of Anchorage's study on the Chester Creek Watershed (Anchorage Waterways Council, 2014).

6.2 Including Effects Due to Sediment

Several empirical methods previously presented involved the knowledge of channel bed makeup and were subsequently not used. Therefore, it is also recommended that this study include the effect of bed material for future method comparisons. Furthermore, the inclusion of bed material could incorporate effects due to sediment transport in channels. Given this, future studies could determine the effect sediment transport has on the change in the roughness coefficient. Sediment transport can change the bedforms of the channel, and even completely wipe away the bed material in the case of high flows, which can then also be recovered by deposition from upstream transport. These dynamic processes could have important ramifications on the changing roughness values for the reach.

6.3 Including Unaccounted for Tributaries

As presented previously, there were two small tributaries connected to the reach in this study. These tributaries were unaccounted for due to time constraints. Consequently, they were visually determined to be negligible. Both tributaries were manmade, naturally dredged channels. It is assumed that both tributaries carry some sort of surface run off because they both originate from

culverts. The tributary upstream had a smaller CSP (corrugated steel pipe) that ran underneath UAA Drive. Its origin is unknown, but it likely feeds into a network of other pipes and manholes for surface runoff in the area. The tributary downstream had a larger winged and grated culvert made of concrete. This culvert looked to have run underneath the NW UAA Parking Lot with an unknown origin. It also most likely fed into a system of other pipes that alleviated surface run off in the UAA campus area.

Although both tributaries are quite small in comparison to the main reach, a more accurate model would still include them. For that reason, it is recommended they be included in future studies.

7.0 References

Anchorage Waterways Council. (2014). *Chester Creek Watershed Plan - Draft (PZC Case No. 2014-0209).* Anchorage, AK: Municipality of Anchorage.

Arcement, G. J., & Schneider, V. R. (1989). *Guide for Selecting Manning's Roughness Coefficients for Natural Channels and Flood Plains (USGS Water-Supply Paper 2339).* USGS.

Boulomytis, V. T., Zuffo, A. C., Filho, D. F., & Imteaz, M. A. (2017). Estimation and calibration of Manning's roughness coefficients for ungauged watersheds on coastal floodplains. *International Journal of River Basin Management*, 199-206.

Coon, W. F. (1998). *Estimation of Roughness Coefficients for Natural Stream Channels with Vegetated Banks (Water-Supply Paper 2441).* Reston, Virginia: U.S. Geological Survey.

Herschy, R. W. (2009). *Streamflow Measurement, Third Edition.* London, England: Routledge: Taylor & Francis Group.

Hicks, D. M., & Mason, P. D. (1998). *Roughness Characteristics of New Zealand Rivers.* Christchurch, New Zealand: Water Resources Publications, LLC.

Hulsing, H., Smith, W., & Cobb, E. D. (1966). *Velocity-Head Coefficients in Open Channels.* USGS.

Oregon Department of Transportation - Highway Division. (2014). *Hydraulics Manual.* Salem, OR.

Strum, T. M. (2009). *Open Channel Hydraulics, Second Edition.* New York, NY: McGraw-Hill Education.

US Army Corps of Engineers. (2016, February). Hydraulic Reference Manual Version 5.0. Davis, CA.

8.0 Appendix

8.1 Chow's Values of the Roughness Coefficient n

Type of channel and description	Minimum	Normal	Maximum
A. Closed Conduits Flowing Partially Full	Minimum	Normal	Maximum
A-1. Metal			
a. Brass, smooth	0.009	0.010	0.013
b. Steel			
1. Lockbar and welded	0.010	0.012	0.014
2. Riveted and spiral	0.013	0.016	0.017
c. Cast Iron			
1. Coated	0.010	0.013	0.014
2. Uncoated	0.011	0.014	0.016
d. Wrought Iron			
1. Black	0.012	0.014	0.015
2. Galvanized	0.013	0.016	0.017
e. Corrugated Metal			
1. Subdrain	0.017	0.019	0.021
2. Stormdrain	0.021	0.024	0.030
A-2. Nonmetal			
a. Lucite	0.008	0.009	0.010
b. Glass	0.009	0.010	0.013
c. Cement			
1. Neat Surface	0.01	0.011	0.013
2. Mortar	0.011	0.013	0.015
d. Concrete			
1. Culvert, straight and free of debris	0.01	0.011	0.013
2. Culvert with bends, connections, and some debris	0.011	0.013	0.014
3. Finished	0.011	0.012	0.014
4. Sewer with manholes, inlet, etc., straight	0.013	0.015	0.017
5. Unfinished, steel form	0.012	0.013	0.014
6. Unfinished, smooth wood form	0.012	0.014	0.016
7. Unfinished, rough wood form	0.015	0.017	0.02
e. Wood			
1. Stave	0.01	0.012	0.014
2. Laminated, treated	0.015	0.017	0.02
f. Clay			
1. Common drainage tile	0.011	0.013	0.017
2. Vitrified sewer	0.011	0.014	0.017
3. Vitrified sewer with manholes, inlet, etc.	0.013	0.015	0.017
4. Vitrified Subdrain with open joint	0.014	0.016	0.018
g. Brickwork			
1. Glazed	0.011	0.013	0.015
2. Lined with cement mortar	0.012	0.015	0.017
h. Sanitary sewers coated with sewage slime with bends and connections	0.012	0.013	0.016
i. Paved invert, sewer, smooth bottom	0.016	0.019	0.02
j. Rubble masonry, cemented	0.018	0.025	0.03

Type of channel and description	Minimum	Normal	Maximum
B. Lined or Built-Up Channels			
B-1. Metal			
a. Smooth steel surface			
1. Unpainted	0.011	0.012	0.014
2. Painted	0.012	0.013	0.017
b. Corrugated	0.021	0.025	0.030
B-2. Nonmetal			
a. Cement			
1. Neat, surface	0.010	0.011	0.013
2. Mortar	0.011	0.013	0.015
b. Wood			
1. Planed, untreated	0.010	0.012	0.014
2. Planed, creosoted	0.011	0.012	0.015
3. Unplaned	0.011	0.013	0.015
4. Plank with battens	0.012	0.015	0.018
5. Lined with roofing paper	0.010	0.014	0.017
c. Concrete			
1. Trowel finish	0.011	0.013	0.015
2. Float finish	0.013	0.015	0.016
3. Finished, with gravel on bottom	0.015	0.017	0.020
4. Unfinished	0.014	0.017	0.020
5. Gunite, good section	0.016	0.019	0.023
6. Gunite, wavy section	0.018	0.022	0.025
7. On good excavated rock	0.017	0.020	
8. On irregular excavated rock	0.022	0.027	
d. Concrete bottom float finish with sides of			
1. Dressed stone in mortar	0.015	0.017	0.020
2. Random stone in mortar	0.017	0.020	0.024
3. Cement rubble masonry, plastered	0.016	0.020	0.024
4. Cement rubble masonry	0.020	0.025	0.030
5. Dry rubble or riprap	0.020	0.030	0.035
e. Gravel bottom with sides of			
1. Formed concrete	0.017	0.020	0.025
2. Random stone mortar	0.020	0.023	0.026
3. Dry rubble or riprap	0.023	0.033	0.036
f. Brick			
1. Glazed	0.011	0.013	0.015
2. In cement mortar	0.012	0.015	0.018
g. Masonry			
1. Cemented rubble	0.017	0.025	0.030
2. Dry rubble	0.023	0.032	0.035
h. Dressed ashlar/stone paving	0.013	0.015	0.017
i. Asphalt			
1. Smooth	0.013	0.013	
2. Rough	0.016	0.016	
j. Vegetal lining	0.030		0.500

Type of channel and description	Minimum	Normal	Maximum
C. Excavated or Dredged			
a. Earth, straight, and uniform			
1. Clean, recently completed	0.016	0.018	0.02
2. Clean, after weathering	0.018	0.022	0.025
3. Gravel, uniform section, clean	0.022	0.025	0.030
4. With short grass, few weeds	0.022	0.027	0.033
b. Earth winding and sluggish			
1. No vegetation	0.023	0.025	0.03
2. Grass, some weeds	0.025	0.030	0.033
3. Dense weeds or aquatic plants in deep channels	0.030	0.035	0.040
4. Earth bottom and rubble sides	0.028	0.030	0.035
5. Stony bottom and weedy banks	0.025	0.035	0.040
6. Cobble bottom and clean sides	0.030	0.040	0.050
c. Dragline-excavated or dredged			
1. No vegetation	0.025	0.028	0.033
2. Light brush on banks	0.035	0.050	0.060
d. Rock cuts			
1. Smooth and uniform	0.025	0.035	0.040
2. Jagged and irregular	0.035	0.040	0.050
e. Channels not maintained, weeds and brush uncut			
1. dense weeds, high as flow depth	0.050	0.080	0.120
2. clean bottom, brush on sides	0.040	0.050	0.080
3. same as above, highest stage of flow	0.045	0.070	0.110
4. dense brush, high stage	0.080	0.100	0.140
D. Natural Streams			
D-1. Minor strams (top width at flood stage <100 ft)			
a. Streams on a plain			
1. Clean, straight, full stage, no rifts or deep pools	0.025	0.030	0.033
2. Same as above, but more stones and weeds	0.030	0.035	0.040
3. Clean, winding, some pools and shoals	0.033	0.040	0.045
4. Same as above, but some weeds and stones	0.035	0.045	0.050
5. Same as above, lower stages, more ineffective slopes and sections	0.040	0.048	0.055
6. Same as 4, but with more stones	0.045	0.050	0.060
7. Sluggish reaches, weedy, deep pools	0.050	0.070	0.080
8. very weedy reaches, deep pools, or floodways with heavy stand of timber and underbrush	0.075	0.100	0.150

Type of channel and description	Minimum	Normal	Maximum
b. Mountain streams, no vegetation in channel, banks usually steep, trees and brush along banks submerged at high stages			
1. Bottom: gravels, cobbles, and few boulders	0.030	0.040	0.050
2. Bottom: cobbles with large boulders	0.040	0.050	0.070
D-2. Floodplains			
a. Pasture, no brush			
1. Short grass	0.025	0.030	0.035
2. High grass	0.030	0.035	0.050
b. Cultivated areas			
1. No crop	0.020	0.030	0.040
2. Mature row crops	0.025	0.035	0.045
3. Mature field crops	0.030	0.040	0.050
c. Brush			
1. Scattered brush, heavy weeds	0.035	0.050	0.070
2. Light brush and trees, in winter	0.035	0.050	0.060
3. Light brush and trees, in summer	0.040	0.060	0.080
4. Medium to dense brush, in winter	0.045	0.070	0.110
5. Medium to dense brush, in summer	0.070	0.100	0.160
d. Trees			
1. Dense willows, summer, straight	0.110	0.150	0.200
2. Cleared land with tree stumps, no sprouts	0.030	0.040	0.050
3. Same as above, but with heavy growth of sprouts	0.050	0.060	0.080
4. Heavy stand of timber, a few down trees, little undergrowth, flood stage below branches	0.080	0.100	0.120
5. Same as 4. with flood stage reaching branches	0.100	0.120	0.160
D-3. Major streams (top width at flood stage >100 ft). The n value is less than that for minor streams of similar description, because banks offer less effective resistance.			
a. Regular section with no boulders or brush	0.025		0.060
b. Irregular and rough section	0.035		0.100

8.2 Observed Cross Sectional Conditions and Hydraulic Properties

Station	Water Surface Elevation (ft)	Flow Area (ft^2)	Wetted Perimeter (ft)	Hydraulic Radius (ft)	Mean Velocity (ft/s)
15	128.05	23.61	20.87	1.131	0.545

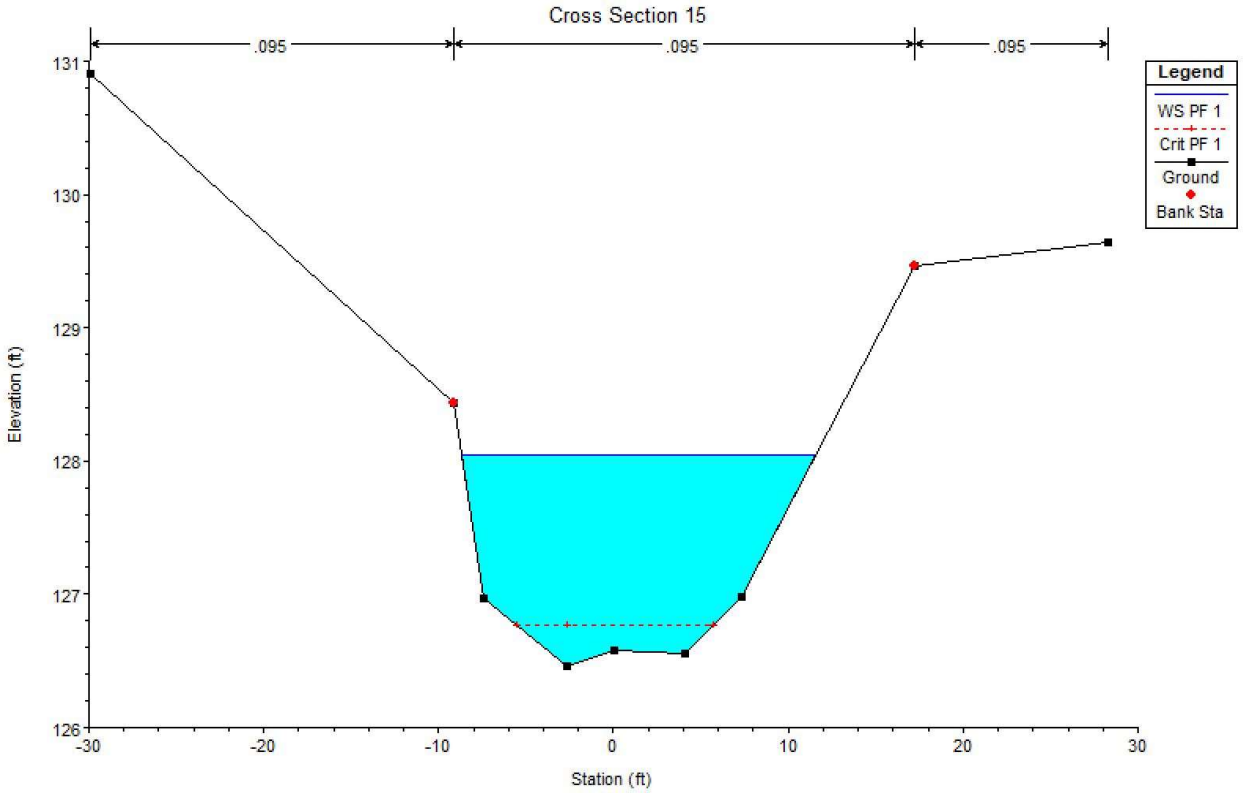

Station	Water Surface Elevation (ft)	Flow Area (ft^2)	Wetted Perimeter (ft)	Hydraulic Radius (ft)	Mean Velocity (ft/s)
14	126.31	5.05	17.09	0.295	2.907

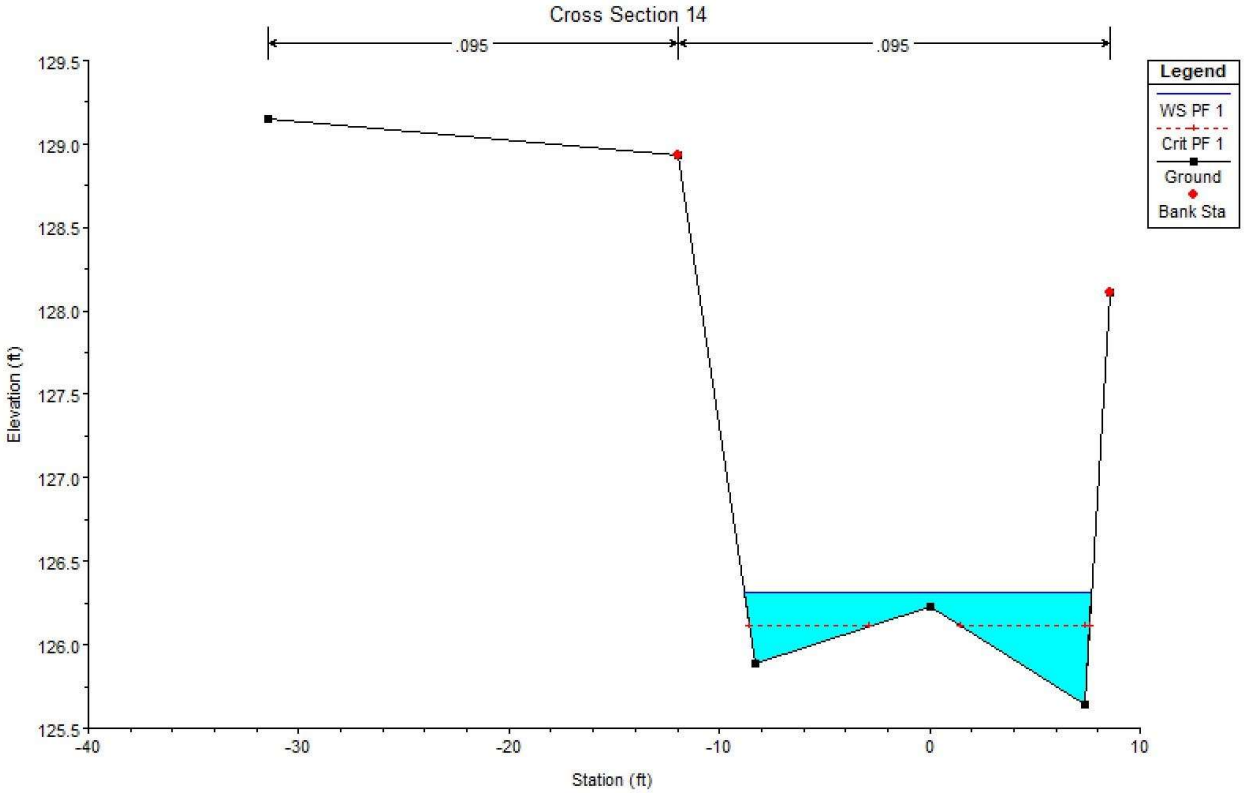

Station	Water Surface Elevation (ft)	Flow Area (ft^2)	Wetted Perimeter (ft)	Hydraulic Radius (ft)	Mean Velocity (ft/s)
13	126.42	14.75	18.72	0.788	0.997

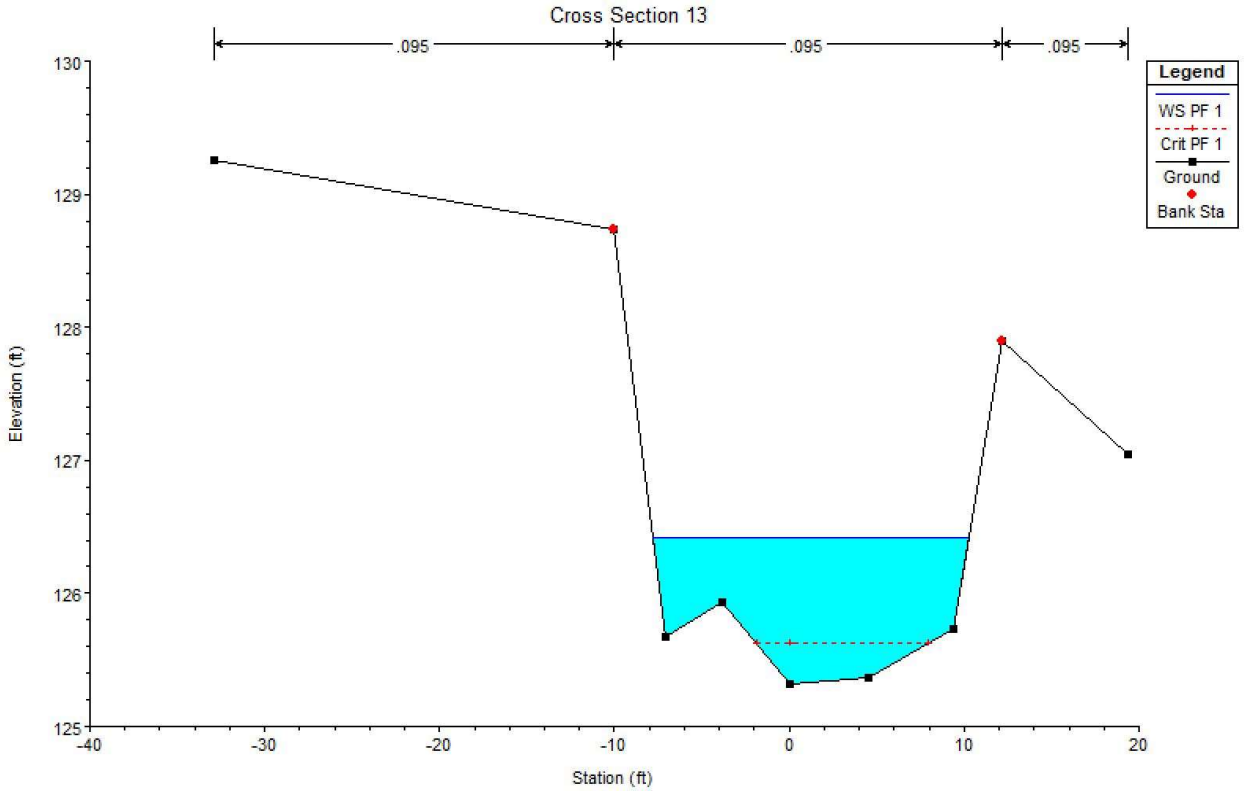

Station	Water Surface Elevation (ft)	Flow Area (ft^2)	Wetted Perimeter (ft)	Hydraulic Radius (ft)	Mean Velocity (ft/s)
12	125.81	16.20	23.01	0.704	1.490

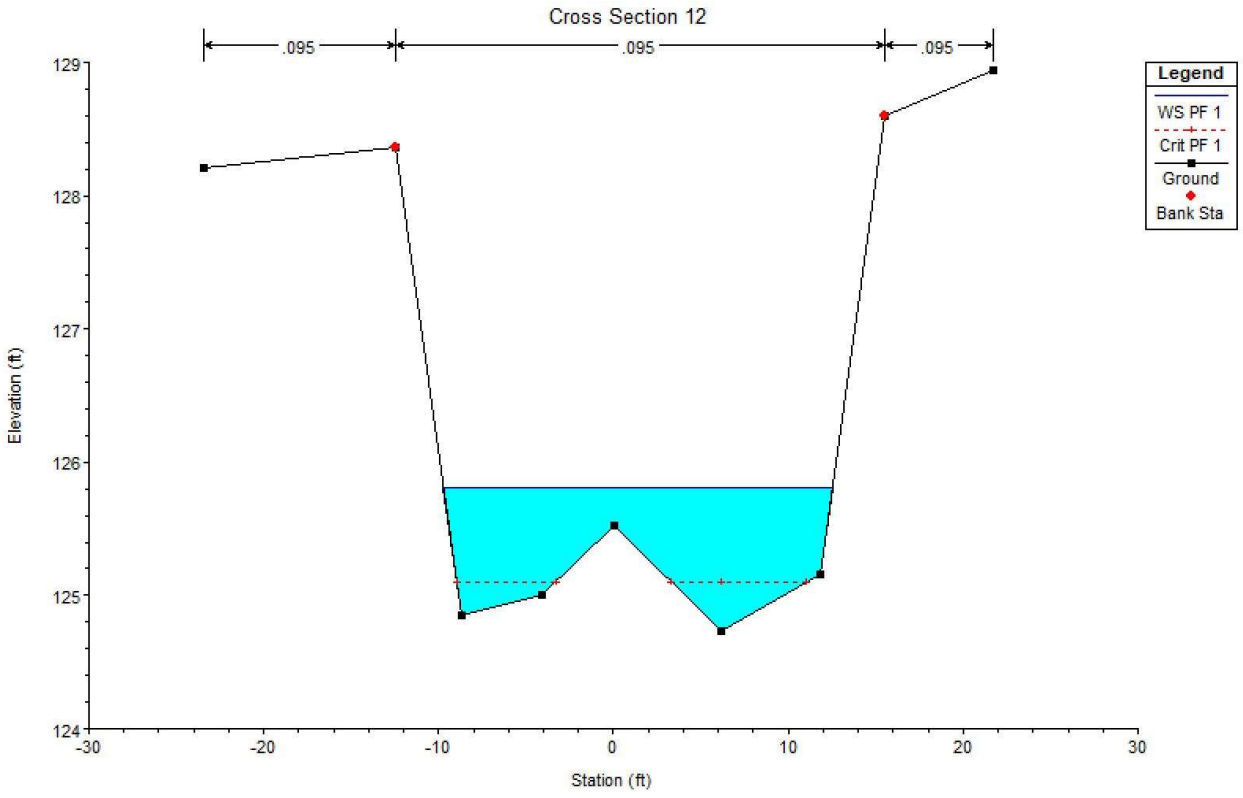

Station	Water Surface Elevation (ft)	Flow Area (ft^2)	Wetted Perimeter (ft)	Hydraulic Radius (ft)	Mean Velocity (ft/s)
11	126.06	27.88	21.17	1.317	0.709

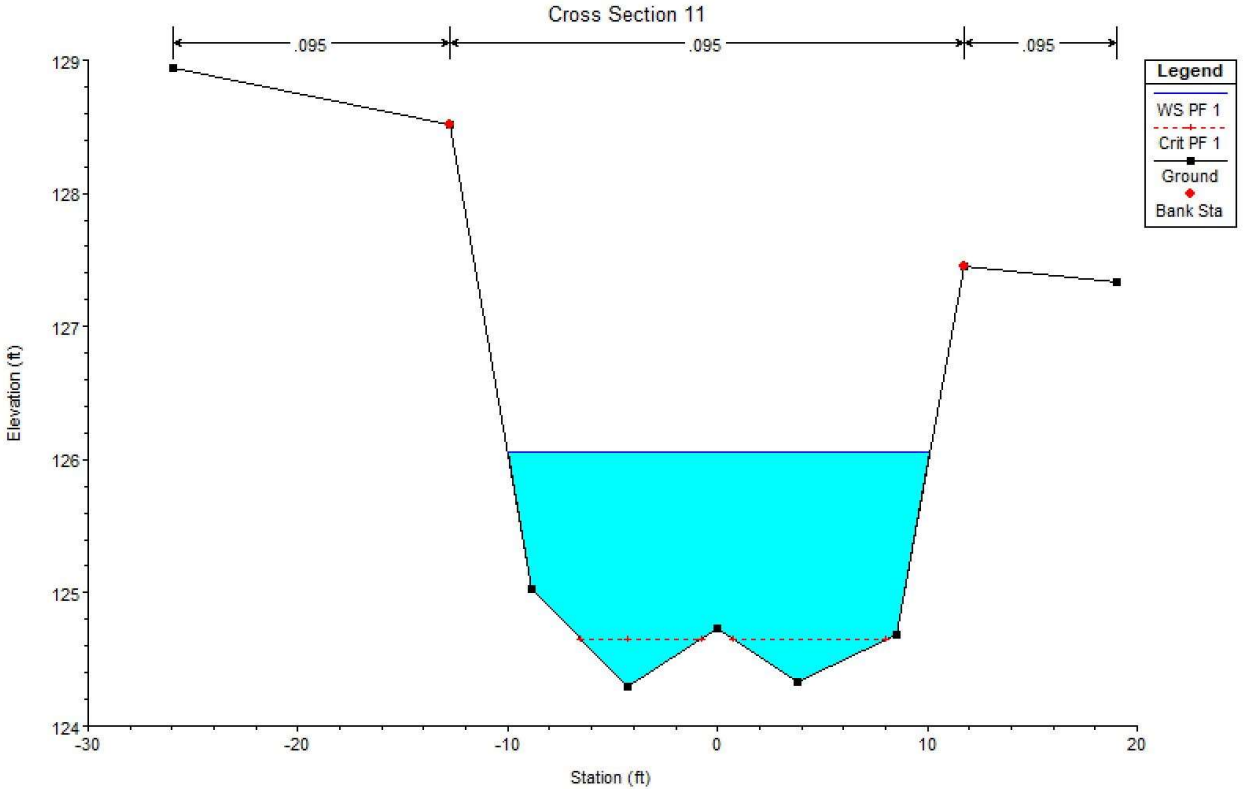

Station	Water Surface Elevation (ft)	Flow Area (ft^2)	Wetted Perimeter (ft)	Hydraulic Radius (ft)	Mean Velocity (ft/s)
10.5	125.49	9.08	13.66	0.665	1.982

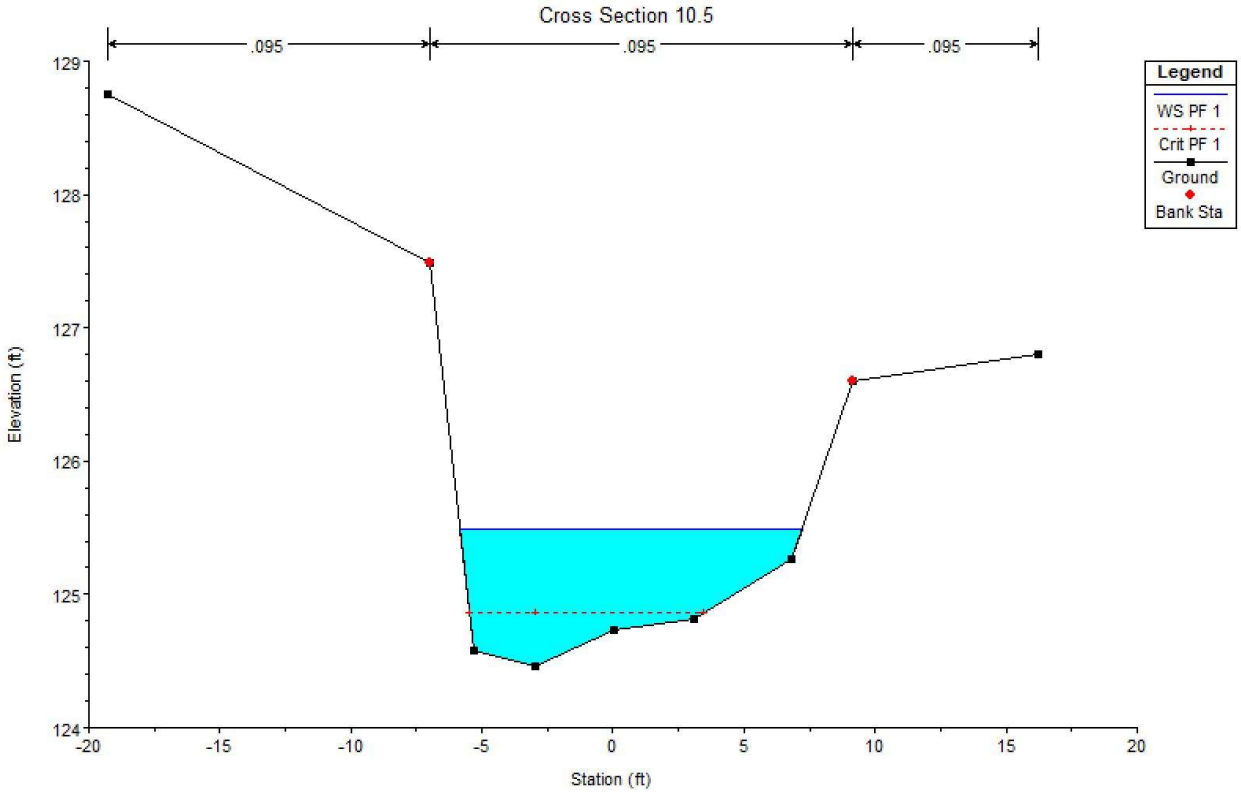

Station	Water Surface Elevation (ft)	Flow Area (ft^2)	Wetted Perimeter (ft)	Hydraulic Radius (ft)	Mean Velocity (ft/s)
10	124.96	9.21	15.75	0.585	1.542

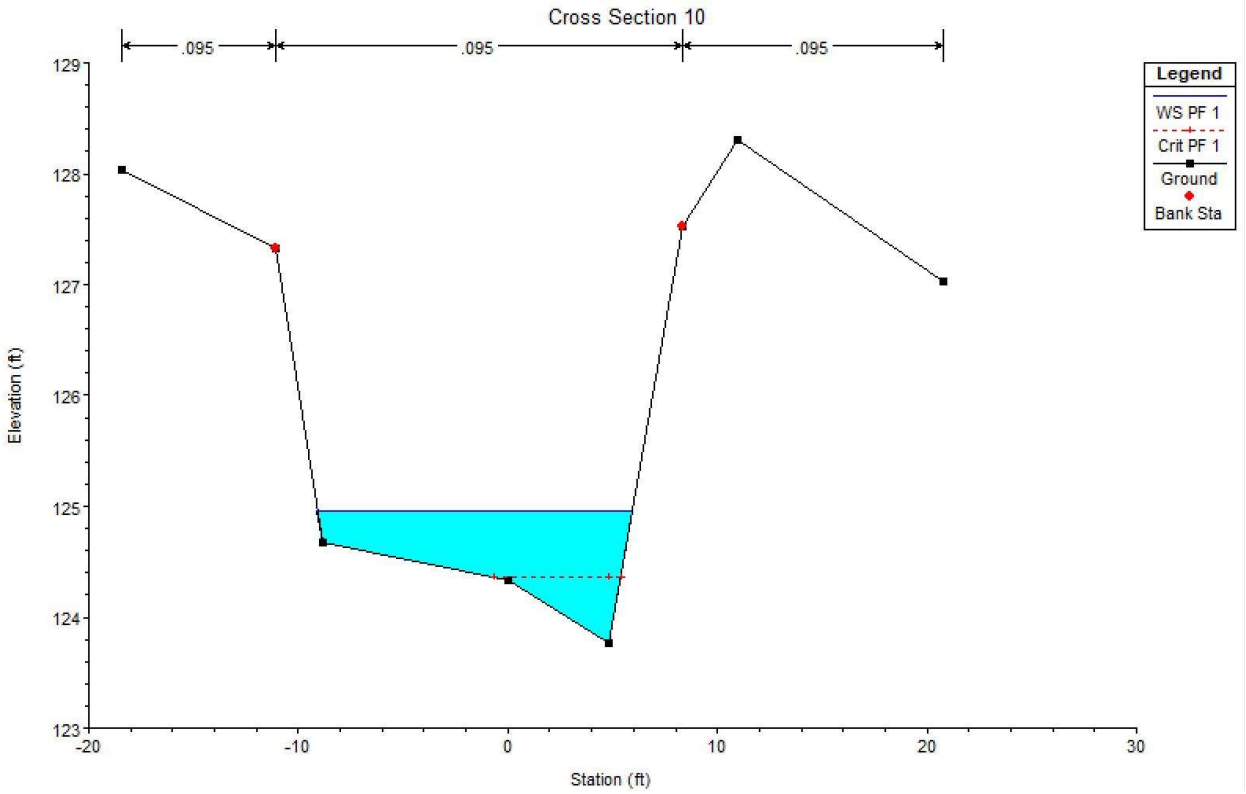

Station	Water Surface Elevation (ft)	Flow Area (ft^2)	Wetted Perimeter (ft)	Hydraulic Radius (ft)	Mean Velocity (ft/s)
9	124.64	22.88	18.54	1.234	1.293

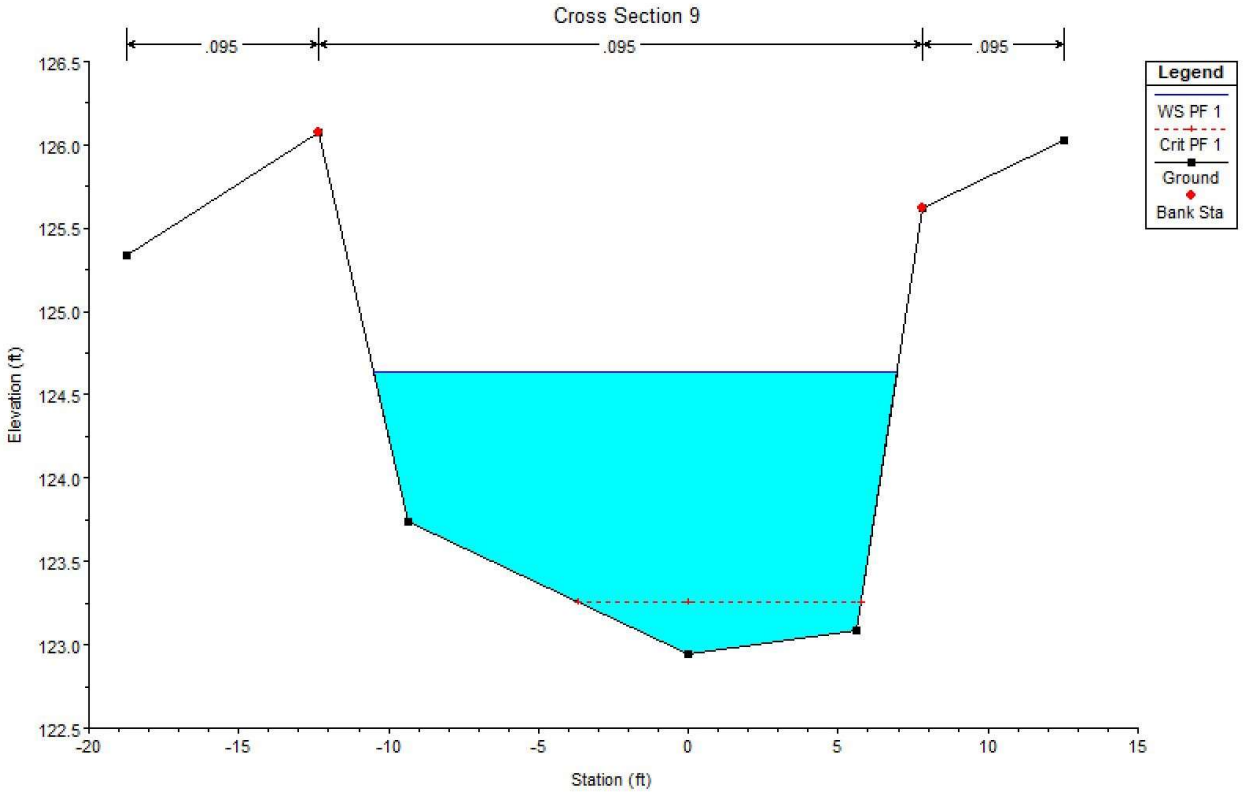

Station	Water Surface Elevation (ft)	Flow Area (ft^2)	Wetted Perimeter (ft)	Hydraulic Radius (ft)	Mean Velocity (ft/s)
8	123.82	13.70	16.15	0.848	2.073

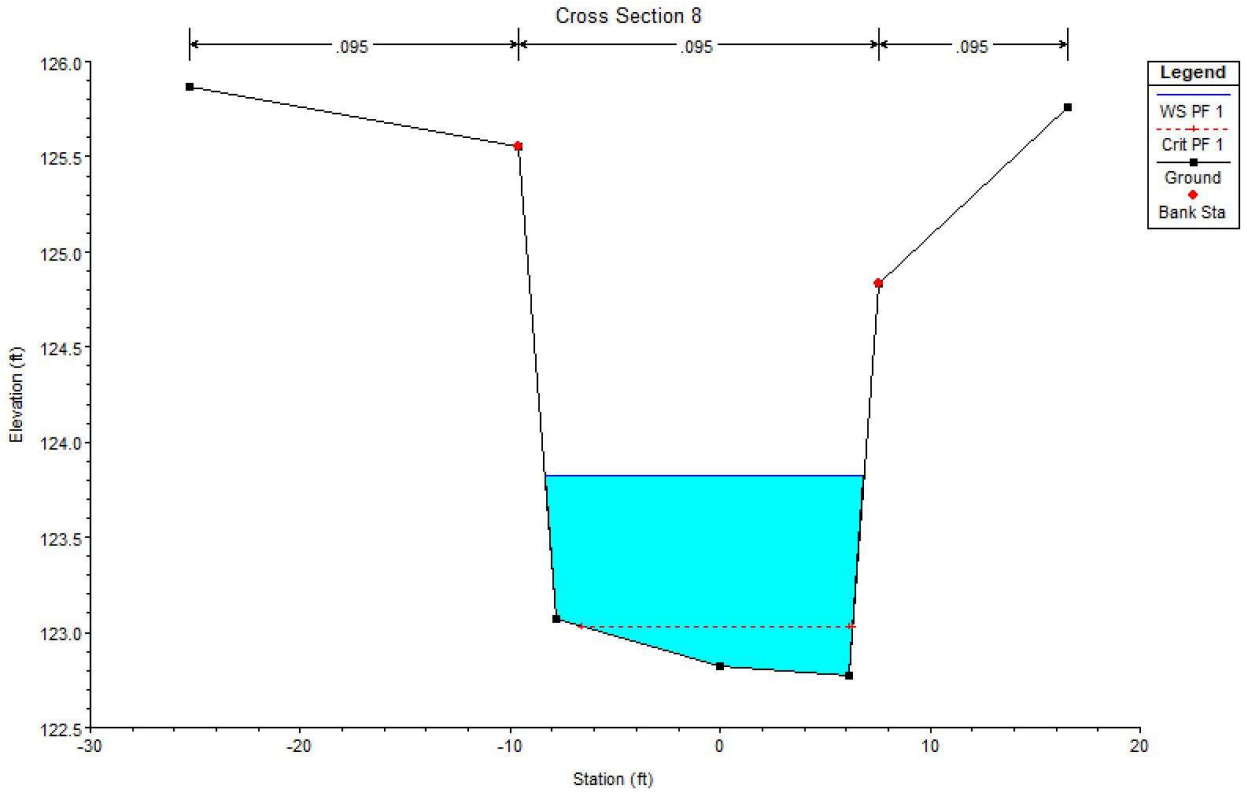

Station	Water Surface Elevation (ft)	Flow Area (ft^2)	Wetted Perimeter (ft)	Hydraulic Radius (ft)	Mean Velocity (ft/s)
7	122.95	7.28	11.32	0.643	1.837

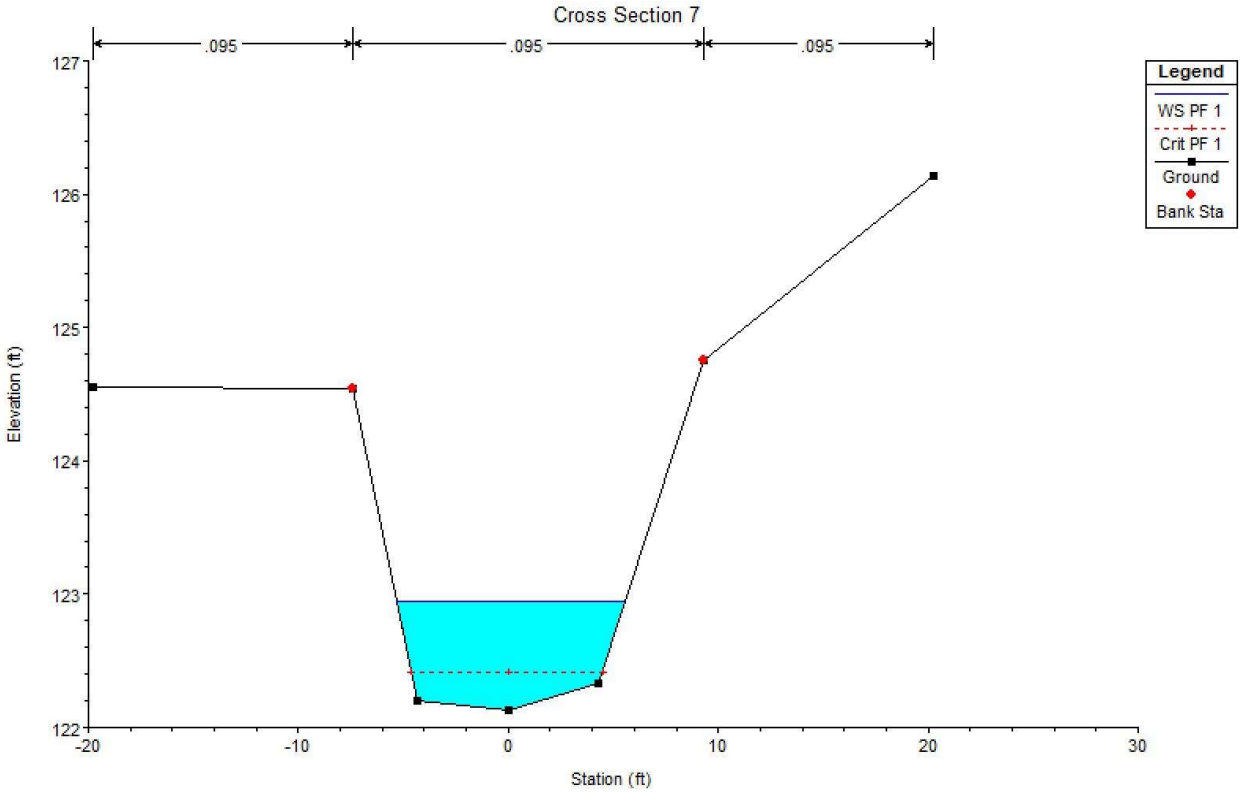

Station	Water Surface Elevation (ft)	Flow Area (ft^2)	Wetted Perimeter (ft)	Hydraulic Radius (ft)	Mean Velocity (ft/s)
6	123.11	15.12	13.20	1.145	0.709

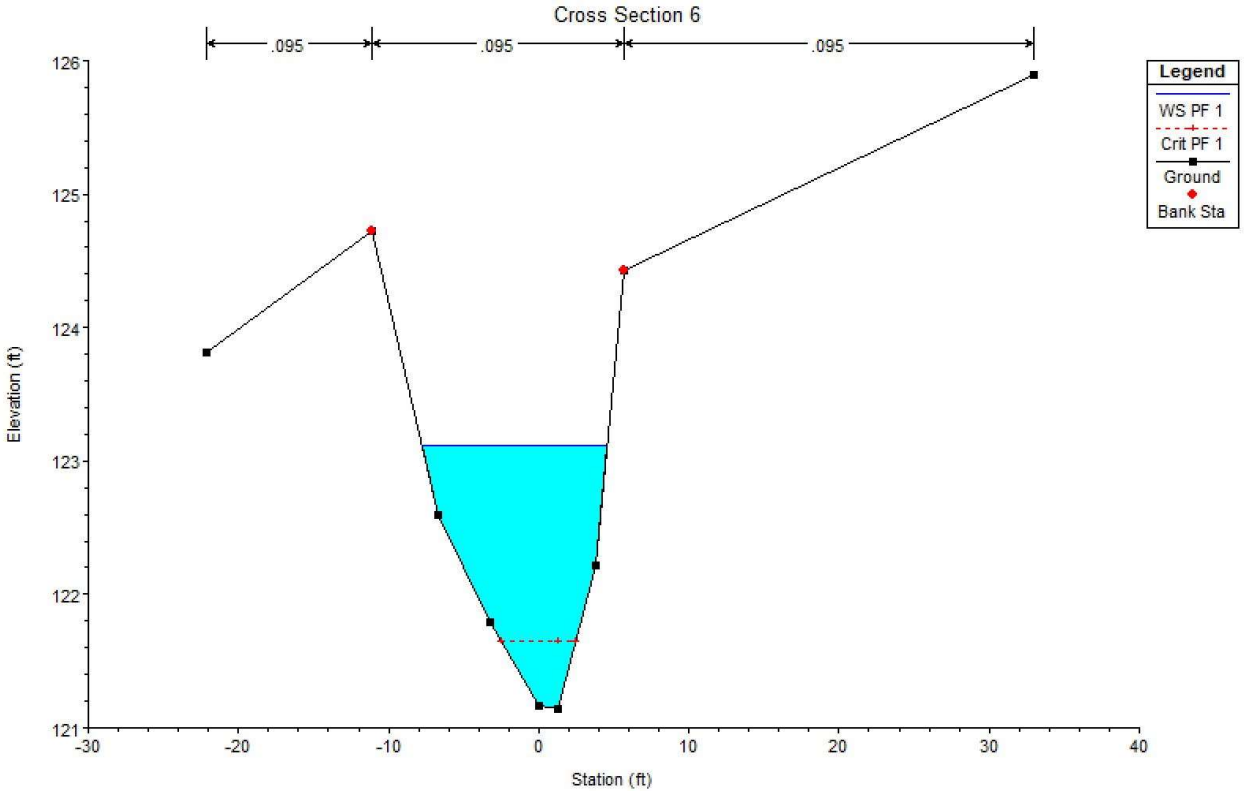

Station	Water Surface Elevation (ft)	Flow Area (ft^2)	Wetted Perimeter (ft)	Hydraulic Radius (ft)	Mean Velocity (ft/s)
5	121.58	12.78	13.95	0.916	1.798

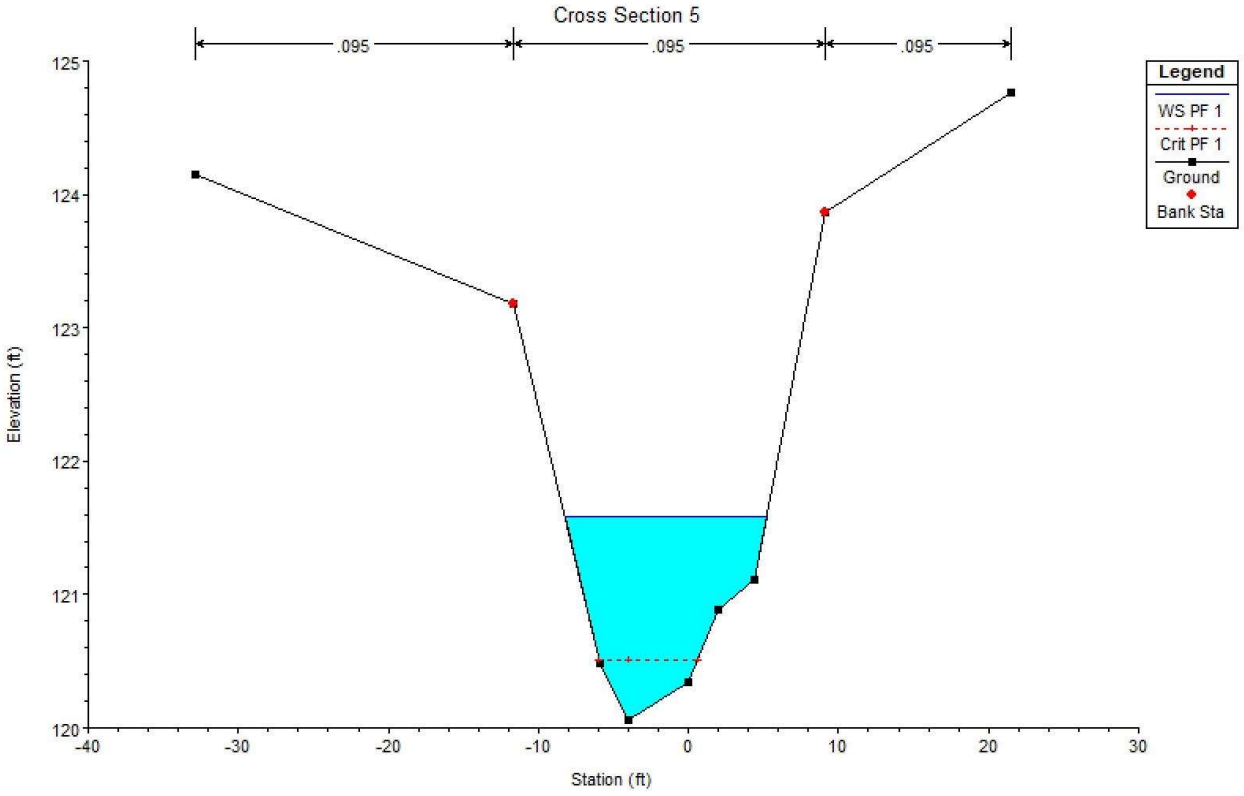

Station	Water Surface Elevation (ft)	Flow Area (ft^2)	Wetted Perimeter (ft)	Hydraulic Radius (ft)	Mean Velocity (ft/s)
4	121.59	11.75	12.17	0.965	1.785

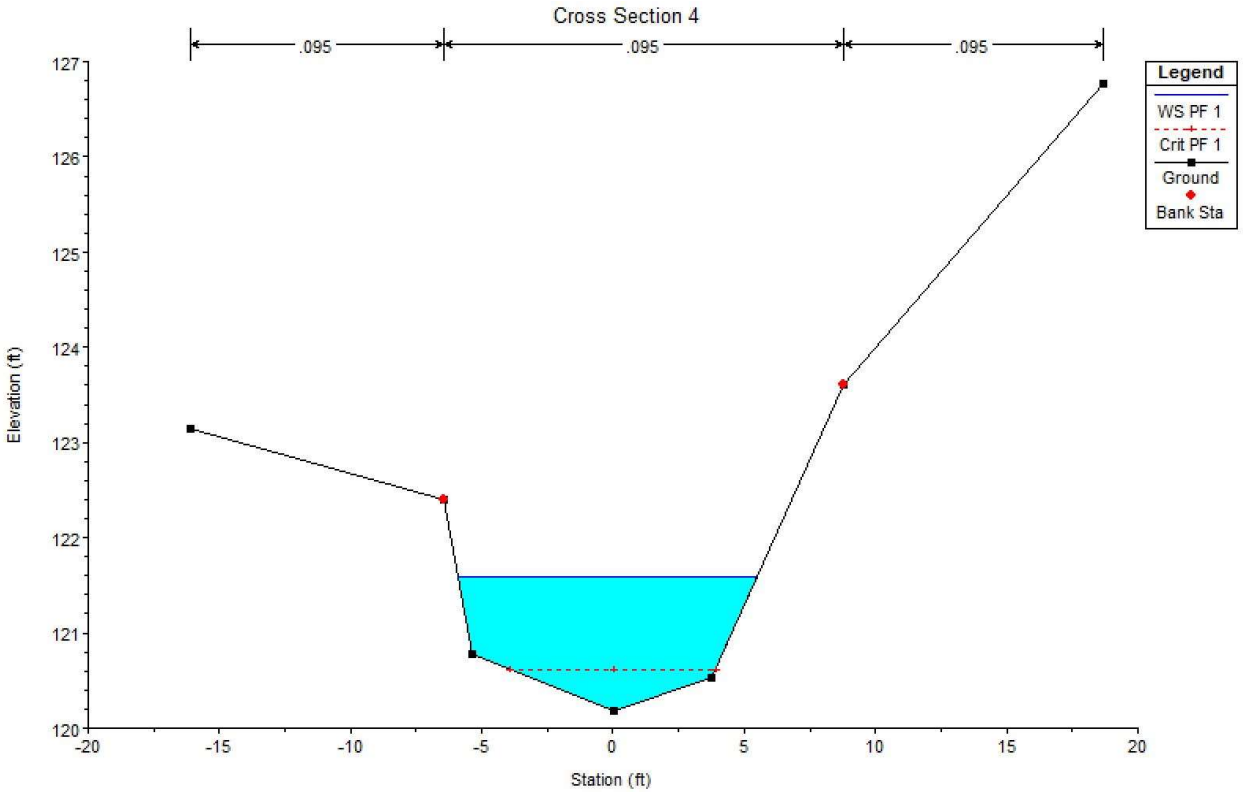

Station	Water Surface Elevation (ft)	Flow Area (ft^2)	Wetted Perimeter (ft)	Hydraulic Radius (ft)	Mean Velocity (ft/s)
3	120.31	6.01	11.48	0.524	1.470

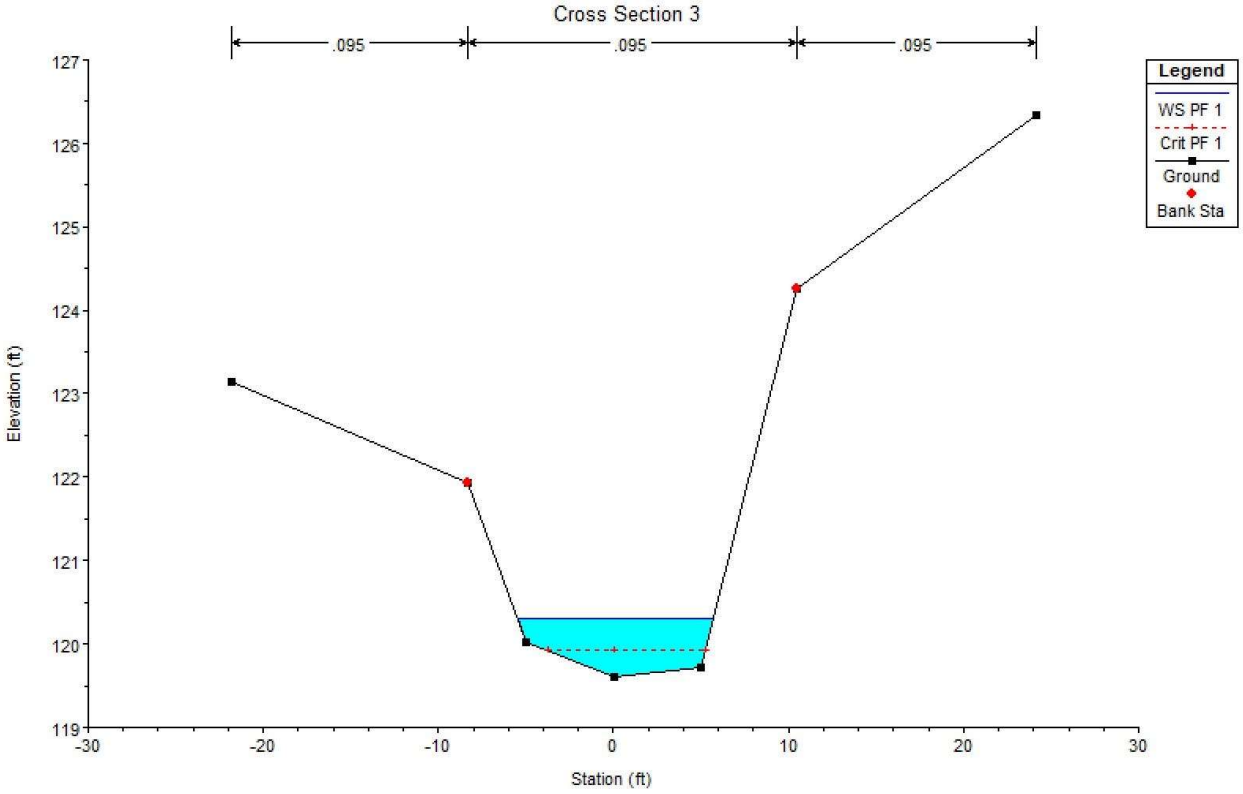

Station	Water Surface Elevation (ft)	Flow Area (ft^2)	Wetted Perimeter (ft)	Hydraulic Radius (ft)	Mean Velocity (ft/s)
2	120.68	20.35	15.10	1.348	1.096

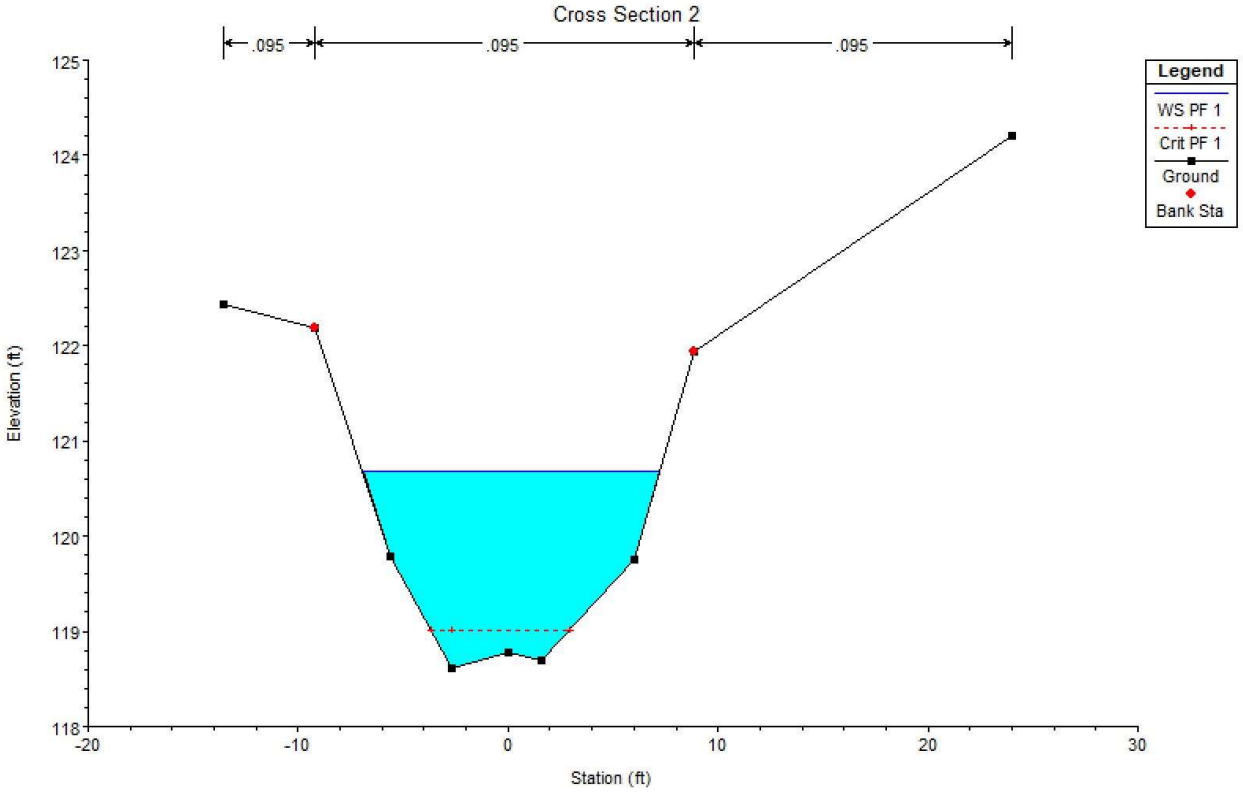

Station	Water Surface Elevation (ft)	Flow Area (ft^2)	Wetted Perimeter (ft)	Hydraulic Radius (ft)	Mean Velocity (ft/s)
1	119.26	5.67	11.15	0.509	1.181

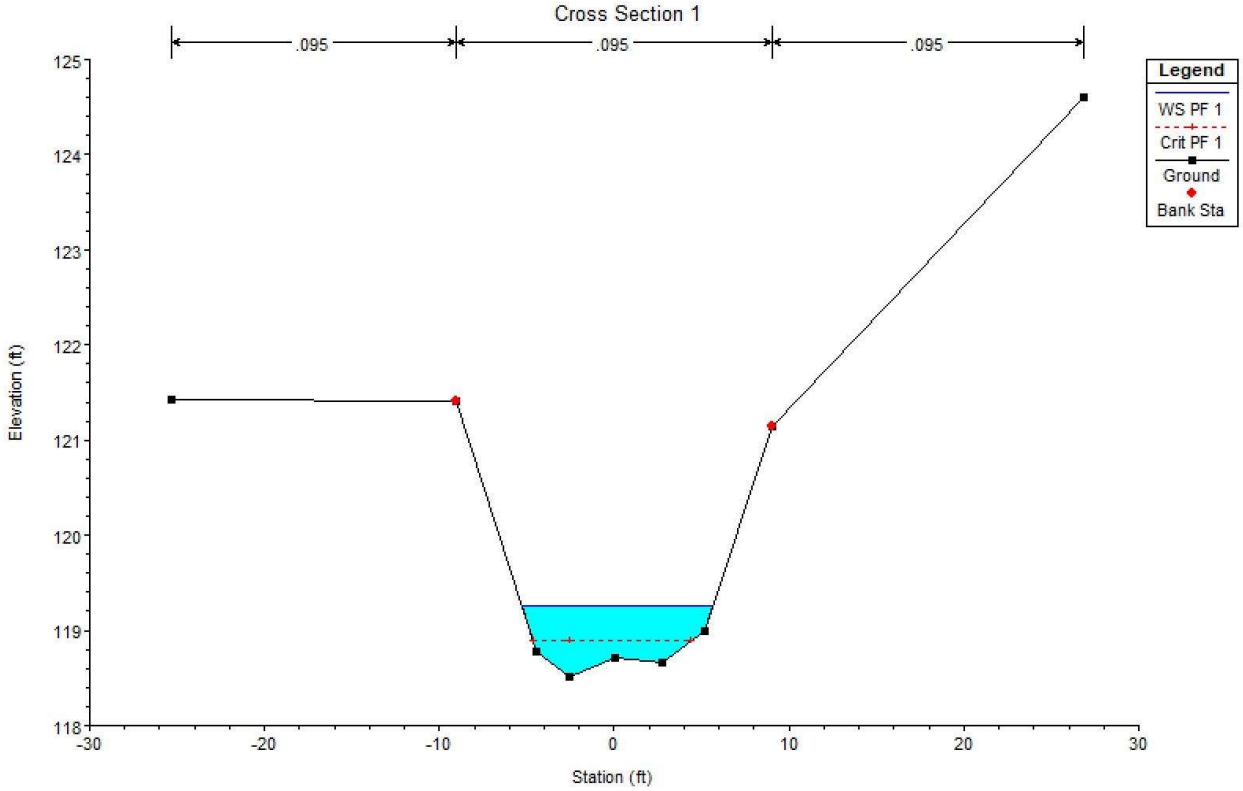

Station	Water Surface Elevation (ft)	Flow Area (ft^2)	Wetted Perimeter (ft)	Hydraulic Radius (ft)	Mean Velocity (ft/s)
0	118.95	14.55	13.40	1.086	1.004